BOUNDARY INTERFERENCE IN A RECTANGULAR WIND TUNNEL WITH PERFORATED WALLS

C. F. Lo and R. H. Oliver
ARO, Inc.

April 1970

PROPULSION WIND TUNNEL FACILITY
ARNOLD ENGINEERING DEVELOPMENT CENTER
AIR FORCE SYSTEMS COMMAND
ARNOLD AIR FORCE STATION, TENNESSEE

NOTICES

When U. S. Government drawings specifications, or other data are used for any purpose other than a definitely related Government procurement operation, the Government thereby incurs no responsibility nor any obligation whatsoever, and the fact that the Government may have formulated, furnished, or in any way supplied the said drawings, specifications, or other data, is not to be regarded by implication or otherwise, or in any manner licensing the holder or any other person or corporation, or conveying any rights or permission to manufacture, use, or sell any patented invention that may in any way be related thereto.

Qualified users may obtain copies of this report from the Defense Documentation Center.

References to named commercial products in this report are not to be considered in any sense as an endorsement of the product by the United States Air Force or the Government.

BOUNDARY INTERFERENCE IN A RECTANGULAR WIND TUNNEL WITH PERFORATED WALLS

C. F. Lo and R. H. Oliver
ARO, Inc.

FOREWORD

The work presented herein was sponsored by the Arnold Engineering Development Center (AEDC), Air Force Systems Command (AFSC), Arnold Air Force Station, Tennessee, under Program Element 63101F, Project A106.

The results of research presented were obtained by ARO, Inc. (a subsidiary of Sverdrup & Parcel and Associates, Inc.), contract operator of AEDC, AFSC, under Contract F40600-69-C-0001. The work was done under ARO Projects PD3014 and PD3914 from January to August, 1969. The manuscript was submitted for publication on February 5, 1970.

Part of this report was submitted by the second author (R. H. Oliver) as a thesis to the University of Tennessee in partial fulfillment of the requirements for the Master of Science degree.

This technical report has been reviewed and is approved.

Charles V. Bennett
Technical Facility
Development Division
Directorate of Plans
and Technology

Harry L. Maynard
Colonel, USAF
Director of Plans
and Technology

ABSTRACT

The boundary interference at subsonic speeds is presented for rectangular wind tunnels with perforated walls. The point-matching method is used for the analysis with an equivalent homogeneous boundary condition at the perforated walls. Numerical results are given for rectangular wind tunnels having various porosities and height-to-width ratios of 1.0, 0.8, and 0.5.

CONTENTS

APPENDIXES

NOMENCLATURE

A_m, B_m, D_m, E_m, G_m, $C1_m$, $C2_m$	Series coefficient constants
b	Semiwidth of test section
C	Cross-sectional area of tunnel
C_D	Drag coefficient
C_L	Lift coefficient
C_m	Complex series coefficient, $B_m + iA_m$, $G_m + iE_m$
d	Doublet strength, U V
h	Semiheight of test section
I_m	Modified Bessel functions of the first kind
K_O, K_1	Modified Bessel functions of the second kind
M	Source strength
M_∞	Free-stream Mach number
n	Outward normal to wall
Q	Porosity parameter, $(1 + \beta/R)^{-1}$
q	Transform parameter
R	Porosity parameter
S	Reference area of model
s	Semispan of wing
U	Free-stream velocity
u	Perturbation velocity in free-stream direction
V	Volume of model
w	Upwash velocity
x, y, z	Cartesian coordinates
x, r, θ	Cylindrical coordinates
β	Compressibility factor, $(1 - M_\infty^2)^{1/2}$
Γ	Circulation about the wing

δ	Lift interference factor, $(C/SC_L) \cdot (w/U_\infty)$
δ_1	Gradient of δ, i. e., streamline curvature factor, $(2\beta hC/SC_L U_\infty) \cdot (\partial w/\partial x)$
ϵ_s	Solid blockage interference, (u_s/U_∞)
ϵ_w	Wake blockage interference, (u_w/U_∞)
λ	Tunnel height-to-width ratio, h/b
ϕ	Perturbation velocity potential
ϕ_i	Interference velocity potential
ϕ_m	Disturbance velocity potential of model
Ω_s	Solid blockage ratio, $\epsilon_s/(\epsilon_s)_c$ (x = 0)
Ω_w	Wake blockage ratio, $\epsilon_w/(\epsilon_w)_c$ (x = 0)

SUBSCRIPTS

c	Closed tunnel
h	Horizontal walls
v	Vertical walls

SECTION I
INTRODUCTION

The development of large, high subsonic speed aircraft requires rather accurate wind tunnel data for aerodynamic design. Testing for such aircraft has normally been performed in transonic wind tunnels which have ventilated test sections such as the transonic wind tunnels at Arnold Engineering Development Center. Historically, the perforated walls were developed to minimize blockage interference at low supersonic Mach numbers by using a nonlifting, cone-cylinder model (Ref. 1). As a result, corrections should be applied to the data for a lifting model to increase accurate data. This fact was pointed out in a recent study of wind tunnel data correlation (Ref. 2) where it was concluded that wind tunnel wall effects must be taken into account to improve the quality of test data.

It is indicated in Ref. 3 that there was no available analytical solution for the boundary interference in a wind tunnel with perforated walls. The only existing solution had been obtained by an electrical analog measurement (Ref. 4) for the case of a square tunnel with four walls perforated.

The purpose of this report is to present an analytical solution of the boundary interference for wind tunnels with perforated walls. The method used in the calculation is the point-matching method in conjunction with Fourier transforms; this method has been used previously in the slotted-wall tunnel (Ref. 5).

The material contained in the report serves to complete the review and extension of boundary interference at subsonic speeds of Ref. 6 by giving results for the case of rectangular tunnels with perforated walls. Finally, based on the theoretical calculations, some optimum configurations are suggested to assist in designing a perforated wall wind tunnel.

SECTION II
GENERAL ANALYSIS

The field equation of an inviscid, irrotational fluid for subsonic flow in terms of the perturbation velocity potential ϕ in cylindrical coordinate is

$$(\beta^2 \frac{\partial^2}{\partial x^2} + \frac{\partial^2}{\partial r^2} + \frac{\partial}{r\partial r} + \frac{\partial^2}{r^2\ \partial\theta^2})\varphi = 0 \qquad (1)$$

The boundary condition for a perforated wall is derived in an average sense by Ref. 7. The average velocity normal to the wall is assumed to be proportional to the pressure drop across the wall. This leads to the boundary condition

$$\frac{\partial \varphi}{\partial x} + \frac{1}{R}\frac{\partial \varphi}{\partial n} = 0 \tag{2}$$

where R is the porosity parameter which is an empirical constant and has been measured in Ref. 1 for a sample of wall. In this report, a related porosity parameter is introduced as

$$Q = \left(1 + \frac{\beta}{R}\right)^{-1} \tag{3}$$

where the value of Q = 0 corresponds to a closed wall and Q = 1 to an open wall.

The linearity of the field equation and its boundary condition permits the perturbation potential to be separated into two parts as

$$\varphi = \varphi_m + \varphi_i \tag{4}$$

where

φ_m = the disturbance potential caused by a model

φ_i = the interference potential induced by the tunnel boundary

A doublet and a source are used in the calculation of solid and wake blockage interference, respectively. A horseshoe vortex is used as the mathematical model for the disturbance potential in the calculation of the lift interference. Since the singularity satisfies Eq. (1), the field equation and boundary conditions for ϕ_i become

$$\left(\beta^2 \frac{\partial^2}{\partial x^2} + \frac{\partial^2}{\partial r^2} + \frac{\partial}{r\partial r} + \frac{1}{r^2}\frac{\partial^2}{\partial \theta^2}\right)\varphi_i = 0 \tag{5}$$

$$\frac{\partial \varphi_i}{\partial x} + \frac{1}{R}\frac{\partial \varphi_i}{\partial n} = -\left(\frac{\partial \varphi_m}{\partial x} + \frac{1}{R}\frac{\partial \varphi_m}{\partial n}\right) \tag{6}$$

The interference potential ϕ_i may be obtained by a Fourier transform in conjunction with the point-matching method (Ref. 5).

For rectangular test sections where the vertical walls and horizontal walls have different porosities, the transformed solution $\bar{\phi}_i$ of

the interference potential may be written as a series solution with undetermined constants in the form

$$\bar{\varphi}_i = \sum_{m=0}^{\infty} \left[C_{1m} \cos m\theta + C_{2m} \sin m\theta \right] I_m \left(\frac{qr}{b}\right) \tag{7}$$

where

$$\bar{\varphi}_i = (2\pi)^{-\frac{1}{2}} \int_{-\infty}^{\infty} \varphi_i \, e^{i \frac{qx}{3b}} \, dx \tag{8}$$

The undetermined constants C_{1m}, C_{2m} are determined by using the transformed boundary conditions

$$- iq \bar{\varphi}_i \pm \frac{b\beta}{R_v} \frac{\partial \bar{\varphi}_i}{\partial y} = - \left(- iq \bar{\varphi}_m \pm \frac{b\beta}{R_v} \frac{\partial \bar{\varphi}_m}{\partial y}\right) \text{ at } y = \pm b \tag{9}$$

$$- iq \bar{\varphi}_i \pm \frac{b\beta}{R_h} \frac{\partial \bar{\varphi}_i}{\partial y} = - \left(- iq \bar{\varphi}_m \pm \frac{b\beta}{R_h} \frac{\partial \bar{\varphi}_m}{\partial y}\right) \text{ at } z = \pm h \tag{10}$$

where

$$\bar{\varphi}_m = (2\pi)^{-\frac{1}{2}} \int_{-\infty}^{\infty} \varphi_m \, e^{i \frac{qx}{\beta b}} \, dx \tag{11}$$

The series solution, Eq. (7), is truncated at a finite term, M. A set of simultaneous linear algebraic equations can be obtained by substituting Eq. (7) into Eqs. (9) and (10) and selecting 2M discrete points uniformly distributed along the boundary. Improved accuracy is achieved, however, by selecting more than 2M points along the boundary and calculating C_{1m}, C_{2m} by satisfying the boundary condition in the least-squares sense. Once the transformed potential, $\bar{\phi}_i$, is obtained, then the interference potential in the physical plane is determined by the inversion formula.

$$\varphi_i = (2\pi)^{-\frac{1}{2}} \int_{-\infty}^{\infty} \bar{\varphi}_i \, e^{-i \frac{xq}{\beta b}} \, dq \tag{12}$$

SECTION III
SOLID BLOCKAGE INTERFERENCE

For solid blockage interference, the model is represented by a three-dimensional doublet. The disturbance potential of the model at the origin in cylindrical coordinates is expressed as

$$\varphi_m(x,r) = \frac{d}{4\pi} \frac{x}{(x^2 + \beta^2 r^2)^{3/2}} \tag{13}$$

The strength of the doublet, d, is related to the model size by the relationship

$$d = U\ V \tag{14}$$

where V is the volume of the model.

Because of the symmetrical property of a rectangular test section and the model disturbance, the transformed solution $\bar{\phi}_i$, Eq. (7) reduces to

$$\bar{\varphi}_i = \sum_{m=0,2,4}^{\infty} C_m\ I_m\ (\frac{qr}{b})\ \cos\ m\theta \tag{15}$$

where

$$C_m = A_m + i\ B_m \tag{16}$$

The transformed model potential, $\bar{\phi}_m$, is

$$\bar{\varphi}_m = i\ \frac{d}{\sqrt{8\pi^3}}\ \frac{q}{\beta b}\ K_o\ (\frac{qr}{b}) \tag{17}$$

The undetermined constants $C_m = A_m + i\ B_m$ may be obtained from the equations given by substituting Eqs. (15) and (17) into the boundary condition Eqs. (9) and (10). The simultaneous equations used to calculate coefficients A_m and B_m by means of the point-matching technique are listed in Appendix I. Then, the interference potential may be obtained from Eqs. (12) and (15) as

$$\varphi_i(x,r,\theta) = \frac{U_\infty V}{2\pi^2\beta^2 b^2} \int_0^\infty \sum_{m=0,2,4}^{\infty} I_m(\frac{qr}{b})\ \cos\ m\theta$$

$$\left[B_m\ \cos\ (\frac{qx}{\beta b}) + A_m\ \sin\ (\frac{qx}{\beta b}) \right]\ q\ dq \tag{18}$$

The solid blockage factor is defined in terms of the interference velocity u_s as

$$\epsilon_s = \frac{u_s}{U} = \frac{1}{U}\frac{\partial \varphi_i}{\partial x} \tag{19}$$

Values of the solid blockage factor ϵ_s (with a constant factor $\beta^3 b^3/V$) and solid blockage ratio $\Omega_s = \epsilon_s/\epsilon_{s,c}$ are presented in Figs. 1 through 3 (Appendix III) for test sections with various height-to-width ratios and all walls of equal porosity. The term $\epsilon_{s,c}$ is the solid blockage factor at the model position for a closed tunnel. For the case of the vertical and horizontal wall porosities being unequal, $Q_v \neq Q_h$, the solid blockage factor for various height-to-width ratios is shown in Fig. 4. It may be seen from Fig. 4 that proper combinations of porosity on the horizontal and vertical walls can be chosen to give zero blockage interference. These combinations are shown in Fig. 5 and indicate the blockage is insensitive to the porosity of vertical walls for the height-to-width ratio less than 0.8.

The longitudinal gradient of the solid blockage factor is expressed as

$$\frac{\partial \epsilon_s}{\partial x} = \frac{1}{U}\frac{\partial u_s}{\partial x} \tag{20}$$

and is shown in Fig. 6 (with a constant factor $\beta^3 b^3/V$) for tunnels with all walls of equal porosity.

SECTION IV
WAKE BLOCKAGE INTERFERENCE

The model used to represent a wake is a three-dimensional point source. The potential of the source in free air is given by

$$\varphi_m(x,r) = -\frac{M}{4\pi\left[x^2 + \beta^2 r^2\right]^{\frac{1}{2}}} \tag{21}$$

where the source strength, M, is related to the model drag by

$$M = \frac{1}{2} U C_D S' \tag{22}$$

The transformed model potential, $\bar{\phi}_m$, is given by

$$\bar{\varphi}_m = - \left(\frac{M}{\pi\sqrt{2\pi}}\right) K_o\left(\frac{qr}{b}\right) \tag{23}$$

The transformed interference potential, $\bar{\phi}_i$, has the same form as for the solid blockage case, Eq. (15). The solution for ϕ_i is found as

$$\varphi_i(x,r,\theta) = \frac{U_\infty C_D S}{2\pi^2 \beta b} \int_0^\infty \sum_{m=0,2,4}^{\infty} I_m\left(\frac{qr}{b}\right) \cos m\theta \left[A_m \cos\left(\frac{qx}{\beta b}\right) - B_m \sin\left(\frac{qx}{\beta b}\right)\right] dq \tag{24}$$

It should be noted that the transformed disturbance potential Eq. (23) is different from that of the solid blockage case, Eq. (17), by a constant factor. Hence, the equations to calculate the coefficients A_m and B_m are the same as those for the solid blockage case listed in Appendix I.

The wake blockage factor is defined as

$$\epsilon_w = \frac{u_w}{U} = \frac{1}{U}\frac{\partial \varphi_i}{\partial x} \tag{25}$$

and the wake blockage ratio Ω_w is defined by $\Omega_w = \epsilon_w/\epsilon_{w,c}$ where $\epsilon_{w,c}$ is the wake blockage factor at x = 0 for the closed tunnel. Results for the wake blockage factor and blockage ratio are shown in Figs. 7 and 8.

The wake blockage factor, ϵ_w (Eq. (25)), approaches zero as $x \to -\infty$ for all $Q > 0$. For $Q = 0$, Eq. (25) gives a finite negative value for ϵ_w as $x \to -\infty$, which is inconsistent with the boundary condition. Therefore, for the case $Q = 0$, a correction must be added to the free-stream potential, shifting the curves for ϵ_w to zero for $x \to -\infty$. Consistent with this, curves of Figs. 7 and 8, which include the closed tunnel case as an endpoint, reflect this discontinuity of the solution as a function of the boundary condition by means of dashed lines near $Q = 0$.

The distribution of wake blockage ratio along the centerline of a tunnel is presented in Fig. 9 for various tunnel height-to-width ratios.

Although the correct values for ϵ_w approach zero as $x \to -\infty$ for all values of Q, the rate at which ϵ_w approaches zero is extremely slow for

values of Q less than about 0.2. Therefore, in application, for a given Q, one should use the value of wake blockage ratio, Ω_w, found by taking the difference between the value of Ω_w at the desired tunnel reference position and the corresponding value of Ω_w at the model position, x = 0.

The wake blockage factor for a square tunnel with various values of porosity of the vertical walls is shown in Fig. 10. The longitudinal gradient of the wake blockage factor

$$\frac{\partial \varepsilon_w}{\partial x} = \frac{1}{U} \frac{\partial u_w}{\partial x} \tag{26}$$

is shown in Fig. 11.

SECTION V
LIFT INTERFERENCE

The lift interference is calculated using a horseshoe vortex to represent the wing model. The potential of the wing with circulation Γ at the origin is given by

$$\varphi_m = \frac{\Gamma s}{2\pi} \frac{\sin \theta}{r} + \frac{\Gamma s}{2\pi} \frac{\sin \theta}{r} \frac{x}{(x^2 + \beta^2 r^2)^{\frac{1}{2}}} = \varphi_{m_1} + \varphi_{m_2} \tag{27}$$

The value Γs is related to the lift of the model by

$$\Gamma s = C_L \, S \, U/4 \tag{28}$$

Since the disturbance potential has been written as two terms, one independent of x and the other dependent on x, the interference potential may be split into two parts as

$$\varphi_i = \varphi_{i_1}(r,\theta) + \varphi_{i_2}(x,r,\theta) \tag{29}$$

The potential ϕ_{i_1}, induced by ϕ_{m_1}, is found as

$$\varphi_{i_1} = \frac{\Gamma s}{2\pi b} \sum_{m=1,3,5}^{\infty} D_m \, r^m \sin m\theta \tag{30}$$

The transformed potential, $\bar{\phi}_{i_2}$, attributable to ϕ_{m_2}, is reduced from Eq. (7)

$$\bar{\varphi}_{i_2} = \sum_{m=1,3,5}^{\infty} C_m \, I_m\left(\frac{qr}{b}\right) \sin m\theta \tag{31}$$

where

$$C_m = G_m + iE_m$$

The transformed potential of ϕ_{m_2} of Eq. (27) is

$$\bar{\varphi}_{m_2} = i(\Gamma s\ \beta/\pi\sqrt{2\pi})\ K_1(\frac{qr}{b})\ \sin\theta \tag{32}$$

The coefficients D_m, G_m, and E_m may be obtained from the equations given by substituting Eqs.(31) and (32) into the boundary condition Eqs. (9) and (10). The equations used to calculate the coefficients by means of the point-matching technique are listed in Appendix II.

The interference potential may be obtained from Eq. (30) and the inverse form of Eq. (31)

$$\varphi_i(x,r,\theta) = \frac{\Gamma s}{2\pi b}\left\{\sum_{m=1,3,5}^{\infty} D_m r^m \sin m\theta + \frac{2}{\pi}\int_0^{\infty}\sum_{m=1,3,5}^{\infty} I_m(\frac{qr}{b})\sin m\theta\left[G_m\cos(\frac{qx}{\beta b}) + E_m\sin(\frac{qx}{\beta b})\right]dq\right\} \tag{33}$$

The lift interference factor, δ, is defined

$$\delta = \frac{C}{S\ C_L}\frac{1}{U}\frac{\partial\varphi_i}{\partial z} \tag{34}$$

and the streamline curvature is defined

$$\delta_1 = \frac{2\ \beta h}{S\ C_L}\frac{C}{U}\frac{1}{U}\left(\frac{\partial^2\varphi_i}{\partial x\ \partial z}\right) \tag{35}$$

The lift interference factor and its distribution along the centerline are shown in Figs. 12 and 13 for tunnels with all walls of equal porosity. Figure 14 shows the lift interference for vertical and horizontal walls of unequal porosities. It may be seen from Fig. 14 that proper combinations of porosity on the horizontal and vertical walls can be chosen to give zero lift interference. These combinations are shown in Fig. 15

and indicate the lift interference, similar to the solid blockage, is insensitive to the porosity of vertical walls for the height-to-width ratio less than 0.8. The streamline curvature at the model position is shown in Fig. 16.

SECTION VI
DISCUSSION AND CONCLUDING REMARKS

All numerical results presented herein were determined by using ten terms of the infinite series and twenty points along one quadrant of the boundary; only one quadrant was required because of the symmetrical property of this problem. In order to examine the accuracy of the present method, the case of closed vertical walls and perforated horizontal walls has been calculated and compared in Ref. 8 with the results obtained in a closed form by another method. The comparison indicates excellent agreement for the case of a square or nearly square tunnel and satisfactory agreement for the case of test sections having height-to-width ratios around 0.5. Similar results have been noted for a slotted wall tunnel as previously reported in Ref. 5.

It is interesting to note that zero interference can be obtained by the proper combination of porosity in the horizontal and vertical walls as shown in Figs. 5 and 15. The solid blockage and lift interference may be eliminated simultaneously at Q_h and Q_v = 0.45 for a square tunnel.

The interference factors are presented for rectangular wind tunnels having various porosities and height-to-width ratios of 1.0, 0.8, and 0.5. The application of these curves to the tunnel data correction may be found in Ref. 6.

REFERENCES

1. Pindzola, M. and Chew, W. L. "A Summary of Perforated Wall Wind Tunnel Studies at the Arnold Engineering Development Center." AEDC-TR-60-9 (AD241573), August 1960.

2. Treon, S. L., Steinle, F. W., Hofstetter, W. R., and Hagerman, J. R. "Data Correlation from Investigation of a High-Subsonic Speed Transport Aircraft Model in Three Major Transonic Wind Tunnels." AIAA Paper No. 69-794, July 1969.

3. Garner, H. C., Rogers, E. W. E., Acum, W. E. A., and Maskell, E. C. "Subsonic Wind Tunnel Wall Corrections." AGARDograph 109, October 1966.

4. Rushton, K. R. and Laing, L. M. "A General Method of Studying Steady Lift Interference in Slotted and Perforated Tunnels." R & M 3567, 1968.

5. Lo, C. F. and Binion, T. W., Jr. "A V/STOL Wind Tunnel Wall Interference Study." AIAA Paper No. 69-171, also J. of Aircraft, Vol. 7, No. 1, Jan.-Feb. 1970, pp 51-57.

6. Pindzola, M. and Lo, C. F. "Boundary Interference at Subsonic Speeds in Wind Tunnels with Ventilated Walls." AEDC-TR-69-47 (AD687440), May 1969.

7. Goodman, T. R. "The Porous Wall Wind Tunnel - Part II - Interference Effect on a Cylindrical Body in a Two-Dimensional Tunnel at Subsonic Speed." CAL Report AD-594-A-3, ATI 94 424, November 1950.

8. Oliver, R. H. "Determination of Blockage and Lift Interference for Rectangular Wind Tunnels with Perforated Walls." Master Thesis, University of Tennessee, Knoxville, Tennessee, August 1969.

APPENDIXES

I. EQUATIONS FOR EVALUATING THE SERIES COEFFICIENTS A_m AND B_m
II. EQUATIONS FOR EVALUATING THE SERIES COEFFICIENTS D_m, G_m, AND E_m
III. ILLUSTRATIONS

APPENDIX I
EQUATIONS FOR EVALUATING THE SERIES COEFFICIENTS A_m AND B_m

The following set of linear algebraic simultaneous equations is used with the point-matching technique to calculate the constant coefficients for the solid blockage and wake blockage interference solutions given in Sections III and IV.

$$\sum_{m=0,2,4}^{M} \left[A_m(1 - Q_v)\left[\frac{mb}{qr}\cos\left[(m-1)\theta\right] I_m\left(\frac{qr}{b}\right)\right.\right.$$

$$\left.\left. + \cos(m\theta)\cos\theta\, I_{m+1}\left(\frac{qr}{b}\right)\right] - B_m Q_v \cos(m\theta) I_m\left(\frac{qr}{b}\right)\right]$$

$$= (1 - Q_v)\cos\theta\, K_1\left(\frac{qr}{b}\right)$$

$$\sum_{m=0,2,4}^{M} \left[A_m Q_v \cos(m\theta) I_m\left(\frac{qr}{b}\right) + B_m(1 - Q_v)\left[\frac{mb}{qr}\cos\left[(m-1)\theta\right] I_m\left(\frac{qr}{b}\right)\right.\right.$$

$$\left.\left. + \cos(m\theta)\cos\theta\, I_{m+1}\left(\frac{qr}{b}\right)\right]\right] = - Q_v K_0\left(\frac{qr}{b}\right)$$

where

$$r = r_v$$

$$\theta = \theta_v$$

$$\sum_{m=0,2,4}^{M} \left[A_m(1 - Q_h)\left[- \frac{mb}{qr}\sin\left[(m-1)\theta\right] I_m\left(\frac{qr}{b}\right)\right.\right.$$

$$\left. + \cos(m\theta)\sin\theta\, I_{m+1}\left(\frac{qr}{b}\right)\right]$$

$$\left. - B_m Q_h \cos(m\theta) I_m\left(\frac{qr}{b}\right)\right] = (1 - Q_h)\sin\theta\, K_1\left(\frac{qr}{b}\right)$$

$$\sum_{m=0,2,4}^{M} \left[A_m Q_h \cos(m\theta) I_m\left(\frac{qr}{b}\right) + B_m(1 - Q_h) \right.$$

$$\left[- \frac{mb}{qr} \sin\left[(m-1)\theta\right] I_m\left(\frac{qr}{b}\right) \right.$$

$$\left. \left. + \cos(m\theta) \sin\theta \; I_{m+1}\left(\frac{qr}{b}\right) \right] \right] = - Q_h K_0\left(\frac{qr}{b}\right)$$

where

$$r = r_h$$

$$\theta = \theta_h$$

APPENDIX II
EQUATIONS FOR EVALUATING THE SERIES COEFFICIENTS D_m, G_m, AND E_m

The following set of equations is used to calculate the constant coefficients for the lift interference solution given in Section V.

$$\sum_{m=1,3,5}^{M} D_m m r^m \sin\left[(m-1)\theta\right] = 2 \sin\theta \cos\theta$$

where

$$r = r_v$$

$$\theta = \theta_v$$

$$\sum_{m=1,3,5}^{M} D_m m r^m \cos\left[(m-1)\theta\right] = -\frac{\sin\theta \cos^2\theta}{\lambda}$$

where

$$r = r_h$$

$$\theta = \theta_h$$

$$\sum_{m=1,3,5}^{M} \left[E_m (1 - Q_v) \left[\frac{mb}{qr} \sin\left[(m-1)\theta\right] I_m\left(\frac{qr}{b}\right) + \sin(m\theta) \cos\theta \, I_{m+1}\left(\frac{qr}{b}\right) \right] - G_m Q_v \sin(m\theta) I_m\left(\frac{qr}{b}\right) \right] = (1 - Q_v) \sin\theta \cos\theta \, K_2\left(\frac{qr}{b}\right)$$

$$\sum_{m=1,3,5}^{M}\left[E_m Q_v \sin(m\theta) I_m\left(\frac{qr}{b}\right) + G_m(1 - Q_v)\left[\frac{mb}{qr}\sin\left[(m-1)\theta\right] I_m\left(\frac{qr}{b}\right) + \sin(m\theta)\cos\theta\, I_{m+1}\left(\frac{qr}{b}\right)\right]\right] = - Q_v \sin\theta\, K_1\left(\frac{qr}{b}\right)$$

where

$$r = r_v$$

$$\theta = \theta_v$$

where

$$\sum_{m=1,3,5}^{M}\left[E_m(1 - Q_h)\left[\frac{mb}{qr}\cos\left[(m-1)\theta\right] I_m\left(\frac{qr}{b}\right) + \sin(m\theta)\sin\theta\, I_{m+1}\left(\frac{qr}{b}\right)\right] - G_m Q_h \sin(m\theta) I_m\left(\frac{qr}{b}\right)\right] = - (1 - Q_h)\left[\frac{b}{qr} K_1\left(\frac{qr}{b}\right) - \sin^2\theta\, K_2\left(\frac{qr}{b}\right)\right]$$

$$\sum_{m=1,3,5}^{M}\left[E_m Q_h \sin(m\theta) I_m\left(\frac{qr}{b}\right) + G_m(1 - Q_h)\left[\frac{mb}{qr}\cos\left[(m-1)\theta\right] I_m\left(\frac{qr}{b}\right) + \sin(m\theta)\sin\theta\, I_{m+1}\left(\frac{qr}{b}\right)\right]\right] = - Q_h \sin\theta\, \dot{K}_1\left(\frac{qr}{b}\right)$$

where

$$r = r_h$$

$$\theta = \theta_h$$

APPENDIX III
ILLUSTRATIONS

The following figures contain the results for the interference factors. In particular, Figs. 1 through 6 contain results for solid blockage interference, Figs. 7 through 11 contain results for wake blockage interference, and Figs. 12 through 16 contain results for lift interference.

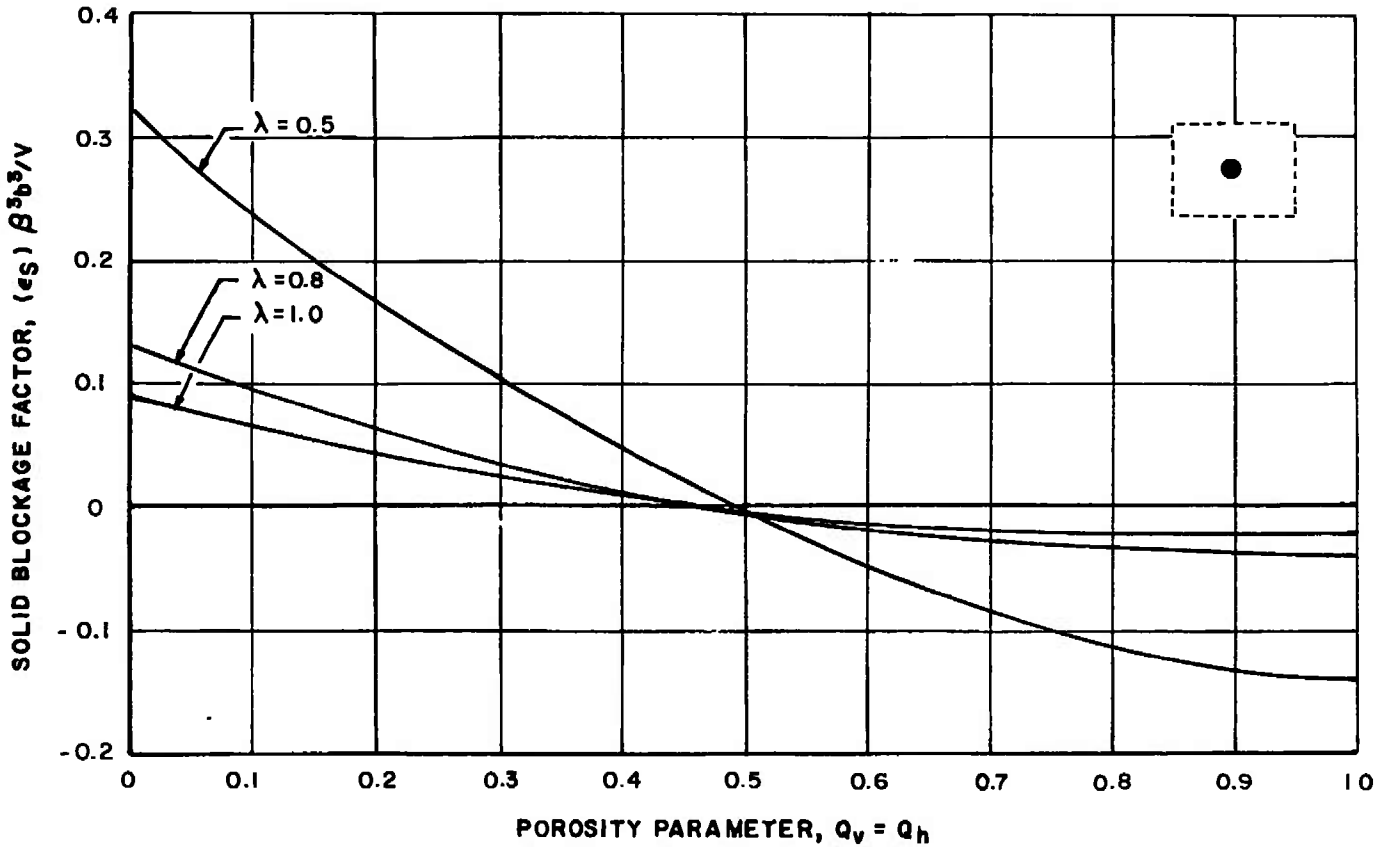

Fig. 1 Solid Blockage Factor at the Model Position for Tunnels with All Walls of Equal Porosity

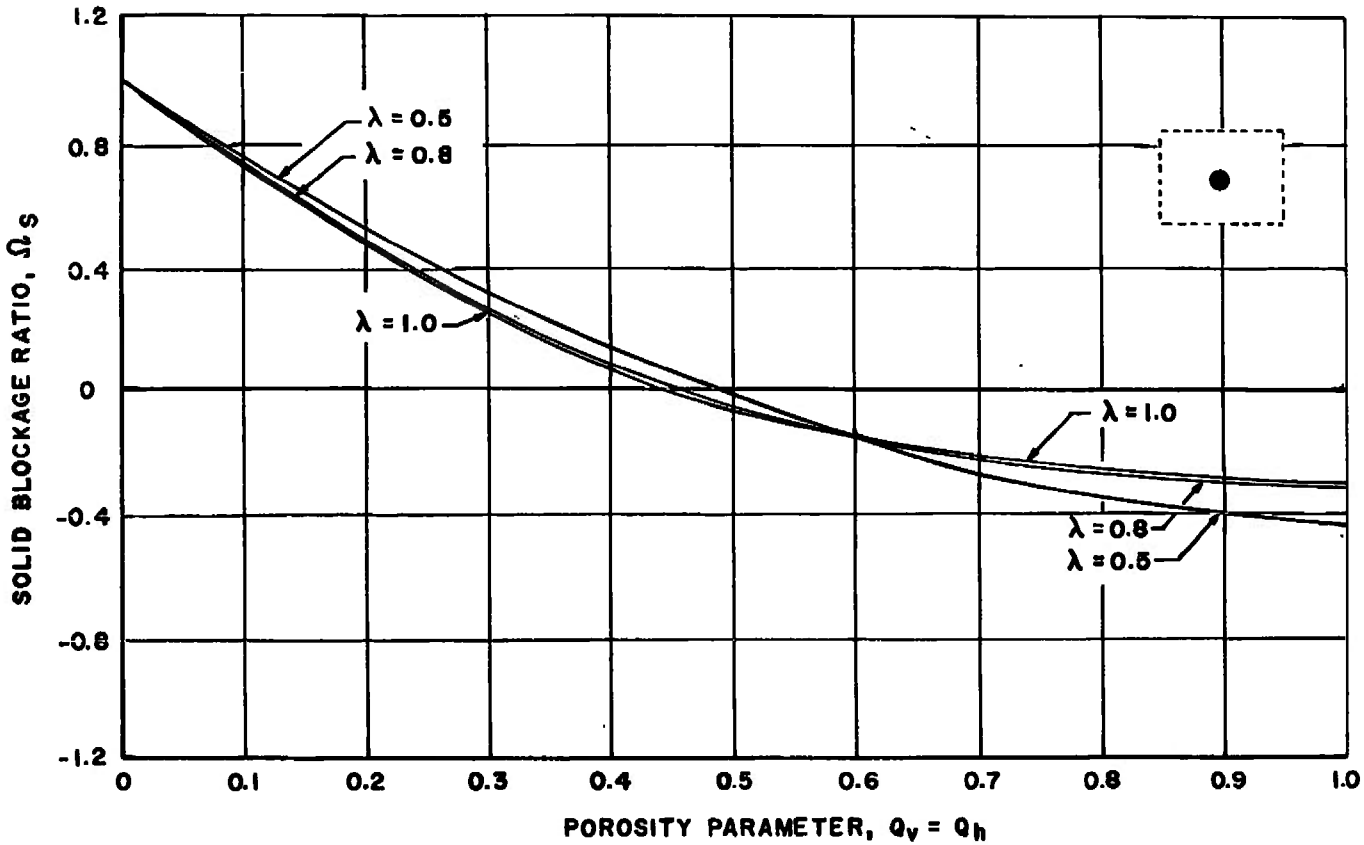

Fig. 2 Solid Blockage Ratio at the Model Position for Tunnels with All Walls of Equal Porosity

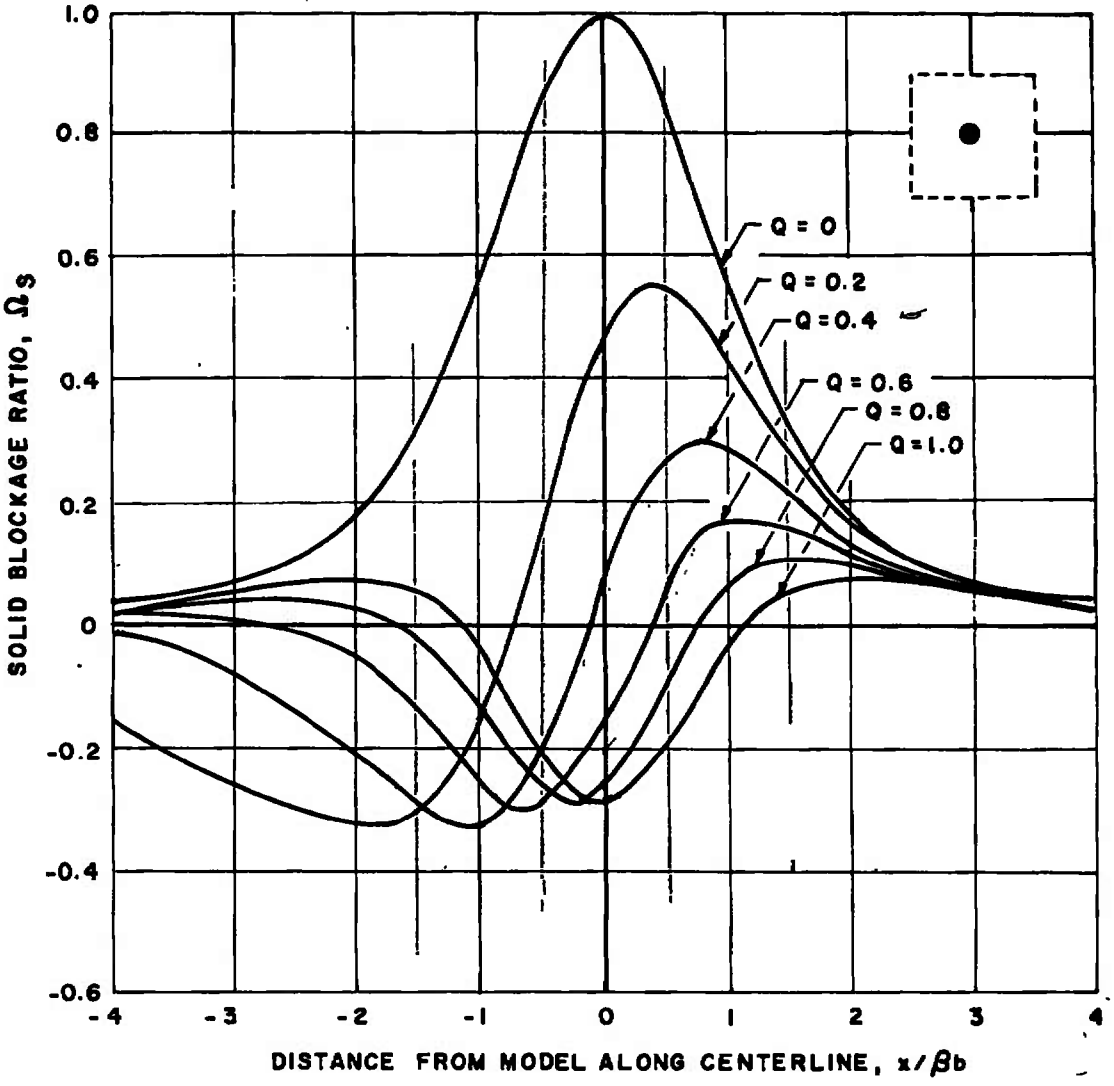

a. $\lambda = 1.0$

Fig. 3 Distribution of the Solid Blockage Ratio along the Centerline of Tunnels with All Walls of Equal Porosity

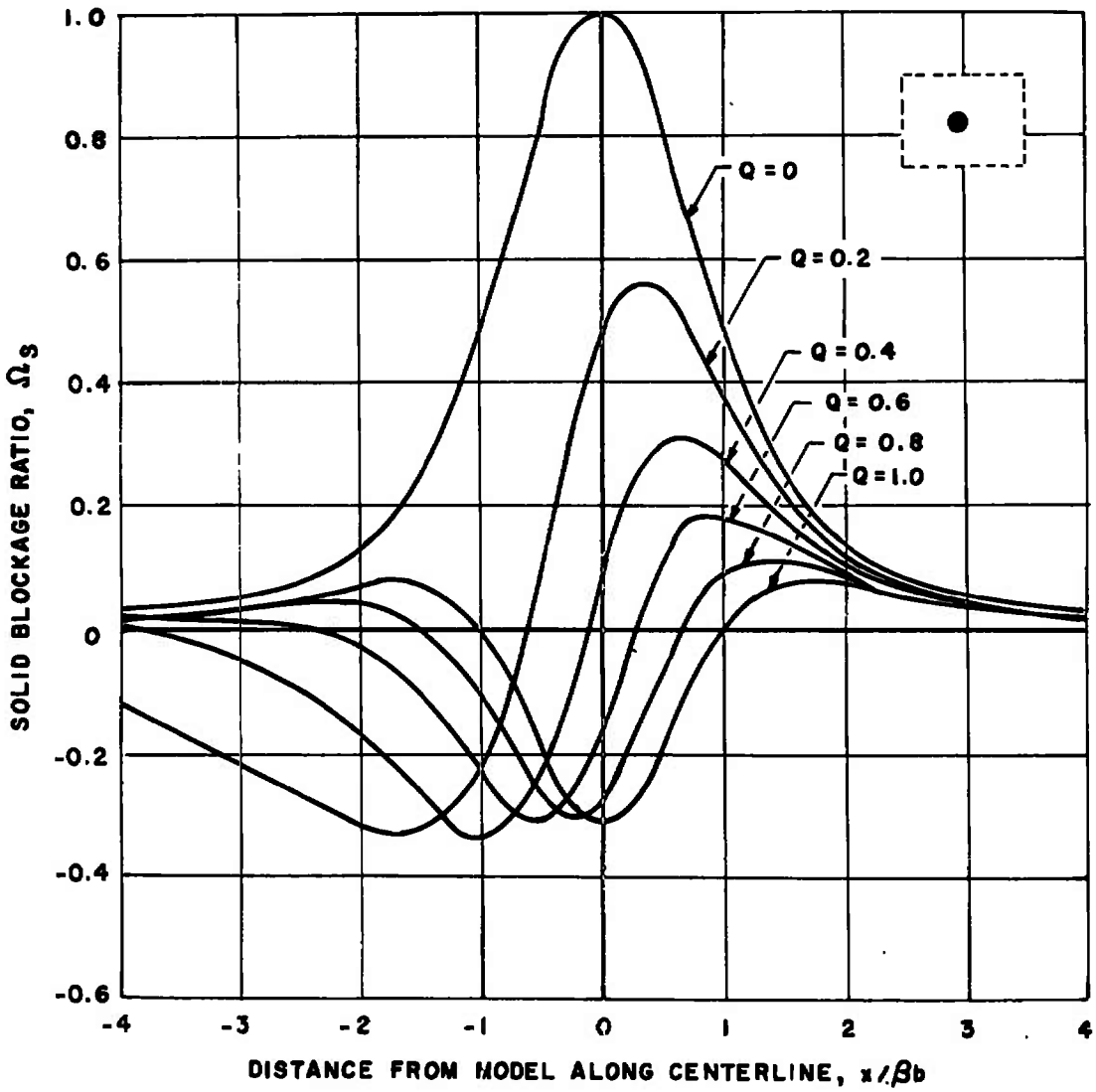

b. $\lambda = 0.8$

Fig. 3 Continued

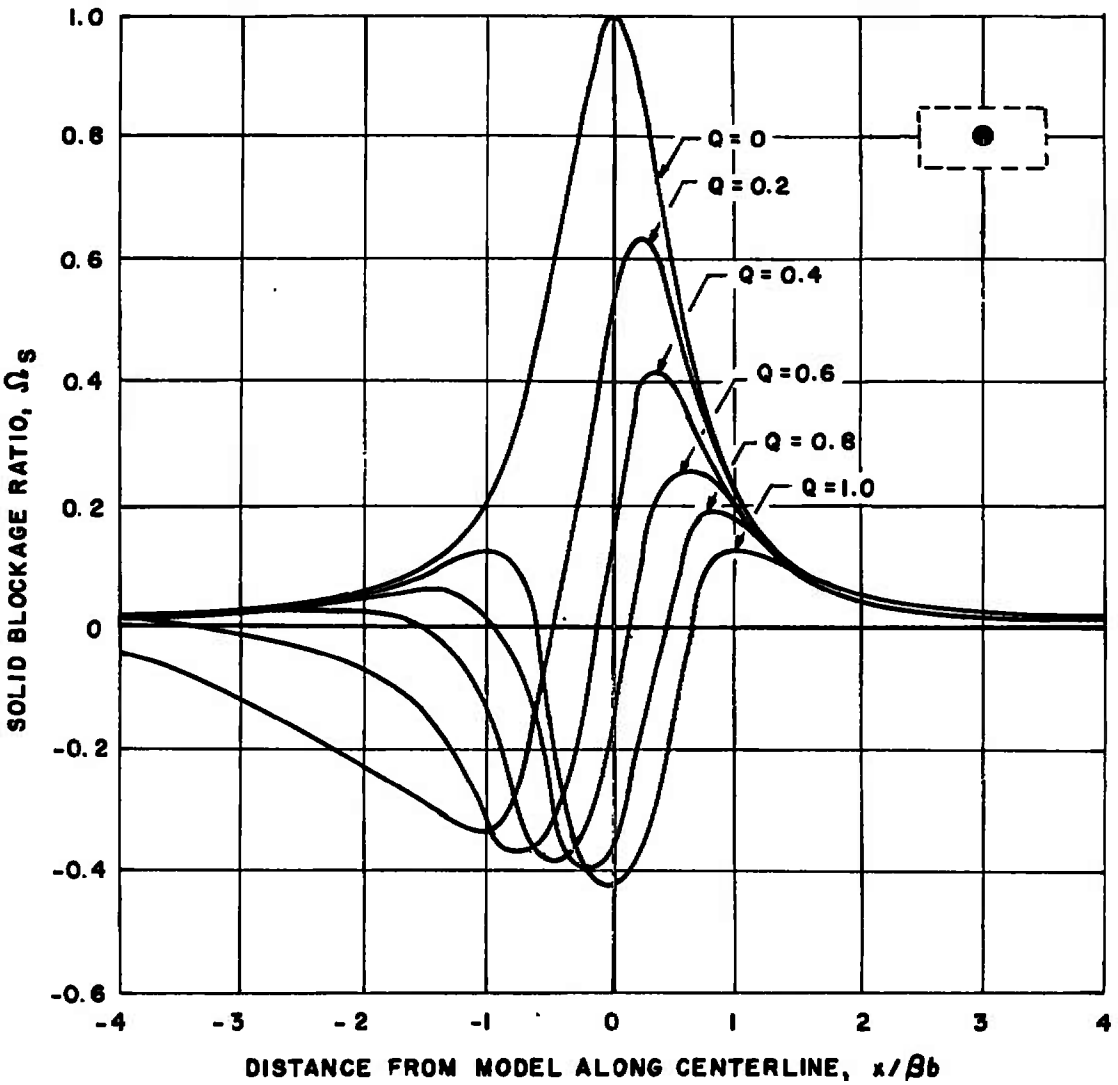

c. $\lambda = 0.5$

Fig. 3 Concluded

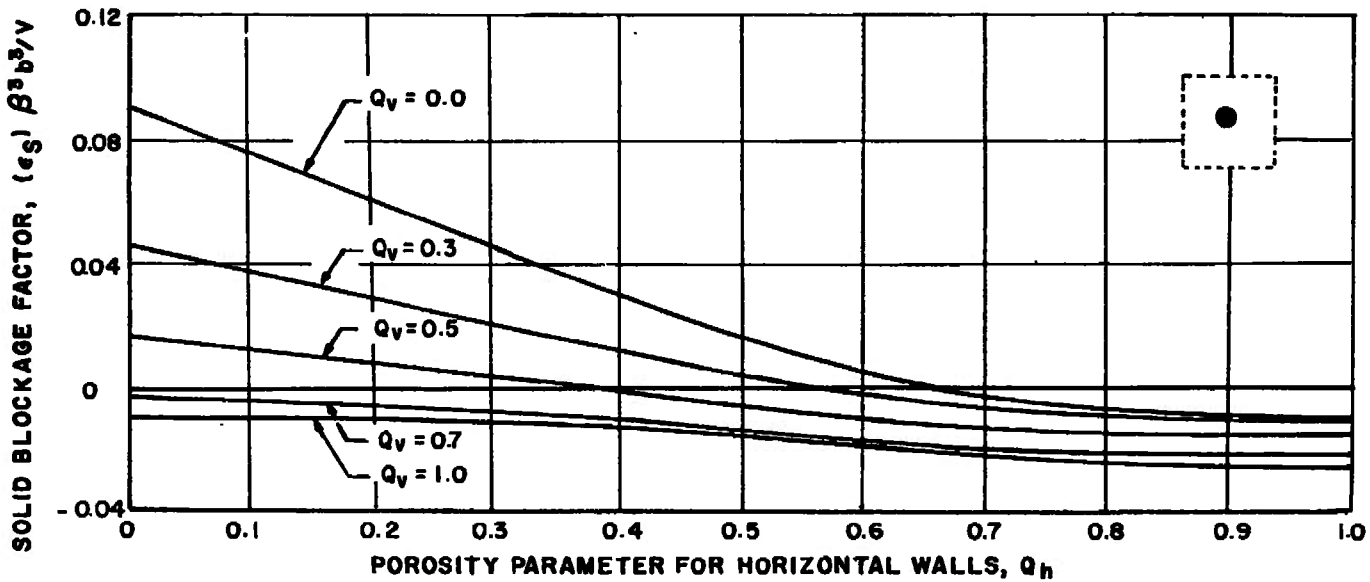

a. $\lambda = 1.0$

Fig. 4 Solid Blockage Factor at the Model Position versus Q_h for Various Values of Q_v

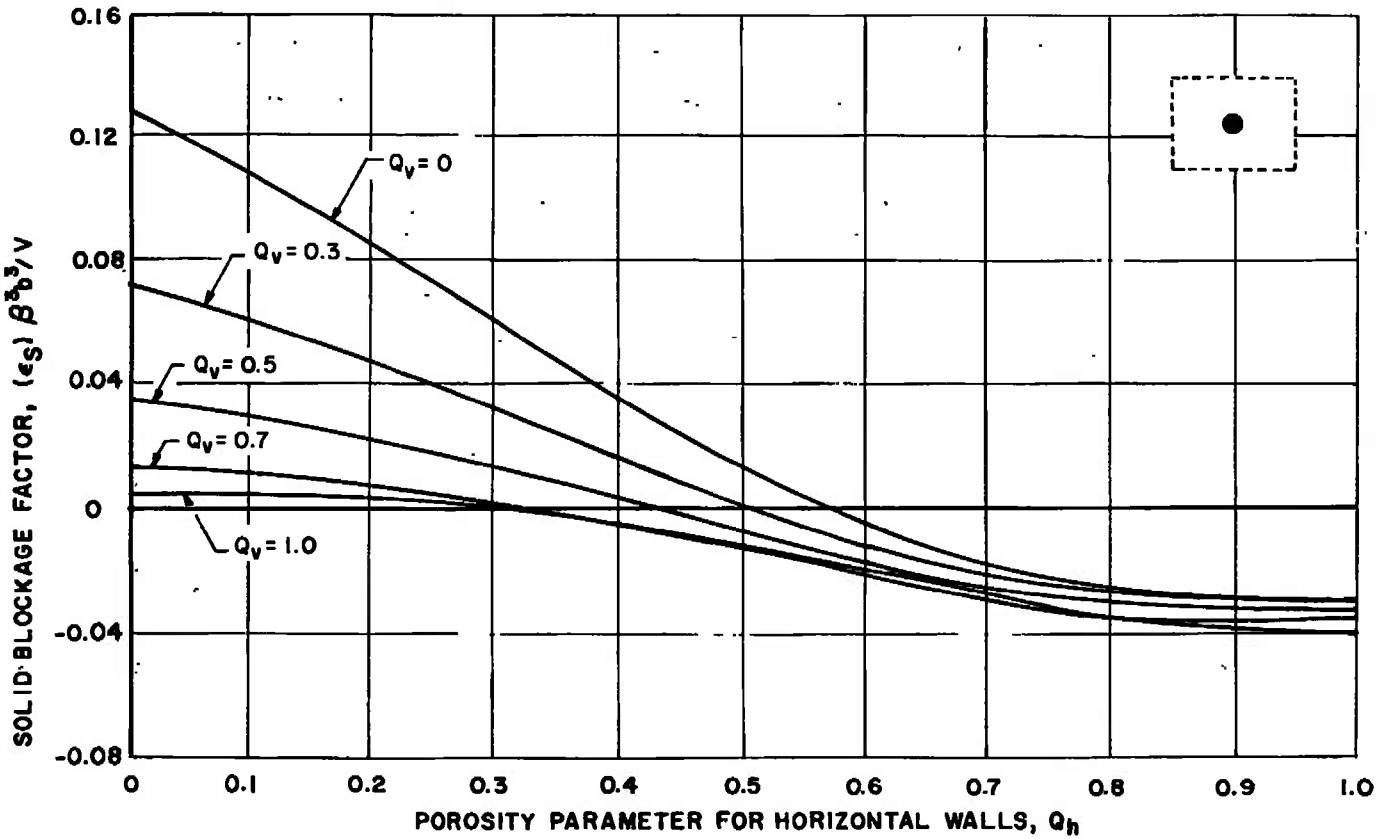

b. $\lambda = 0.8$

Fig. 4 Continued

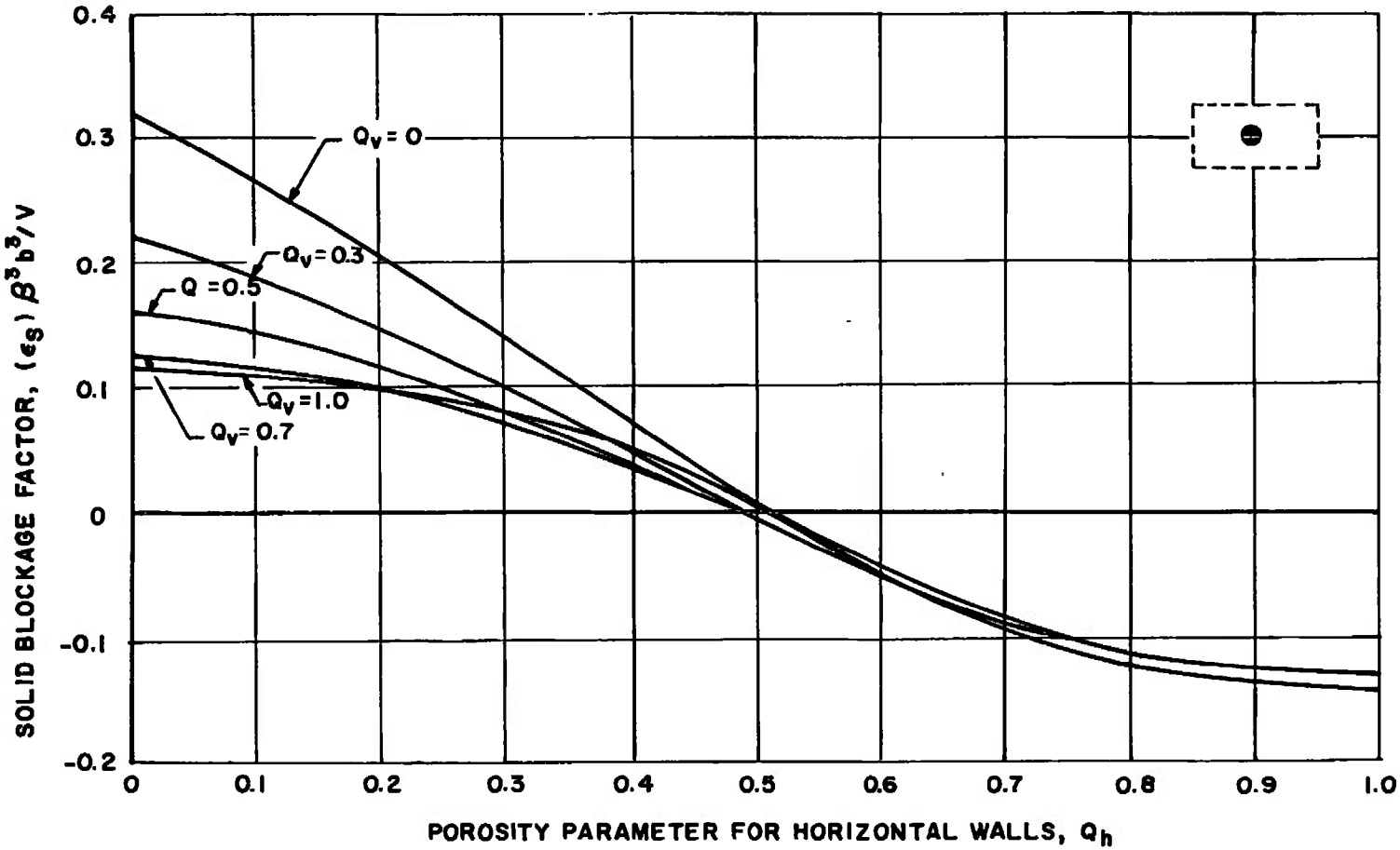

c. $\lambda = 0.5$

Fig. 4 Concluded

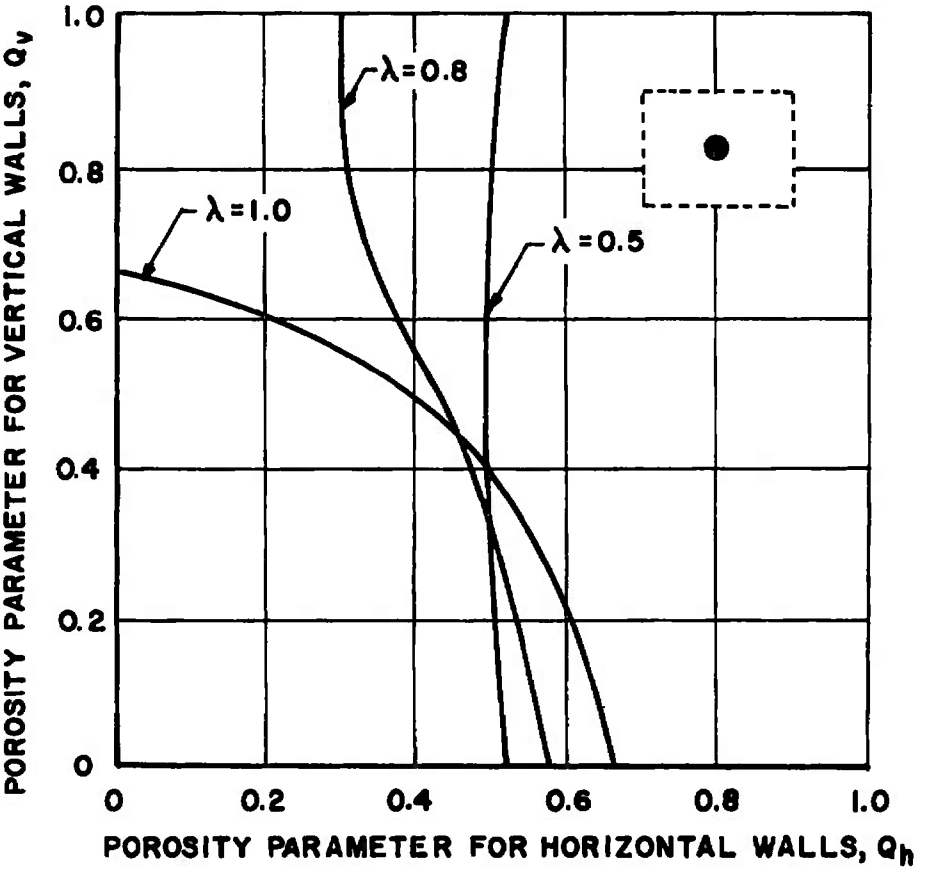

Fig. 5 Zero Solid Blockage Interference Curves for Perforated Tunnels

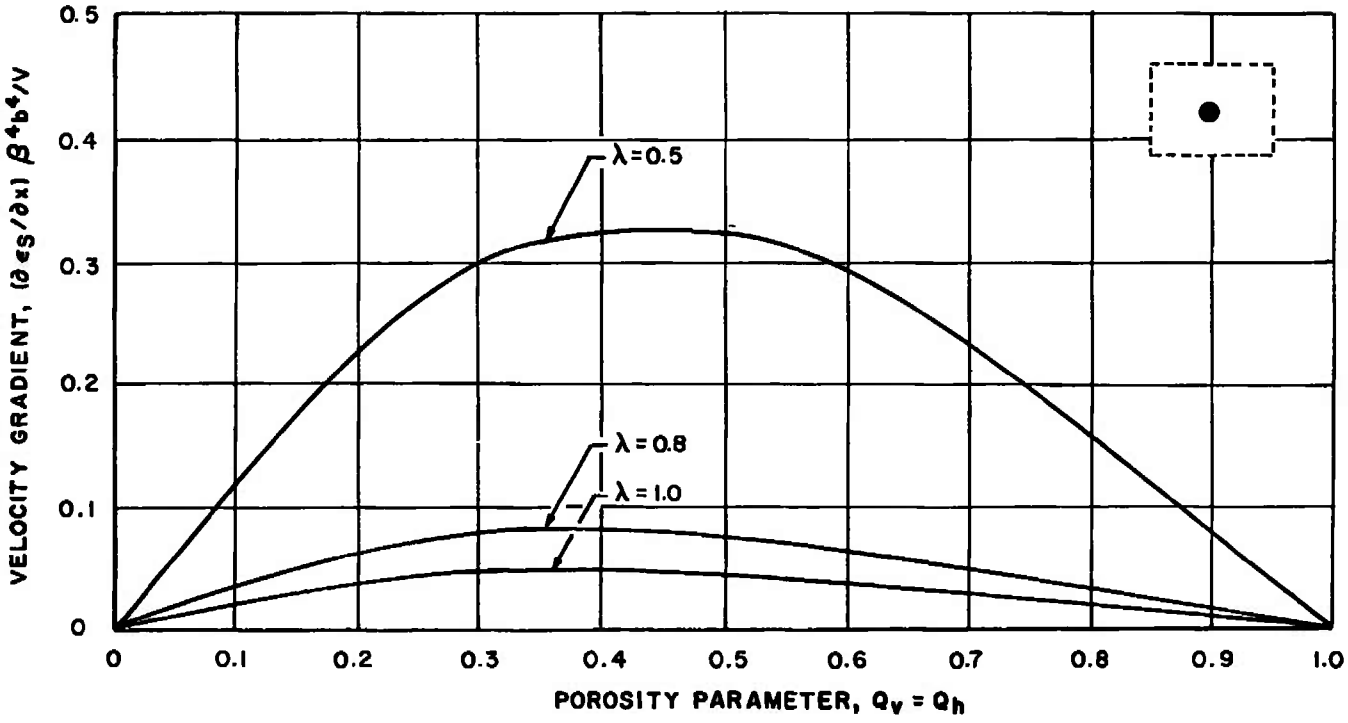

Fig. 6 Solid Blockage Gradient at the Model Position for Tunnels with All Walls of Equal Porosity

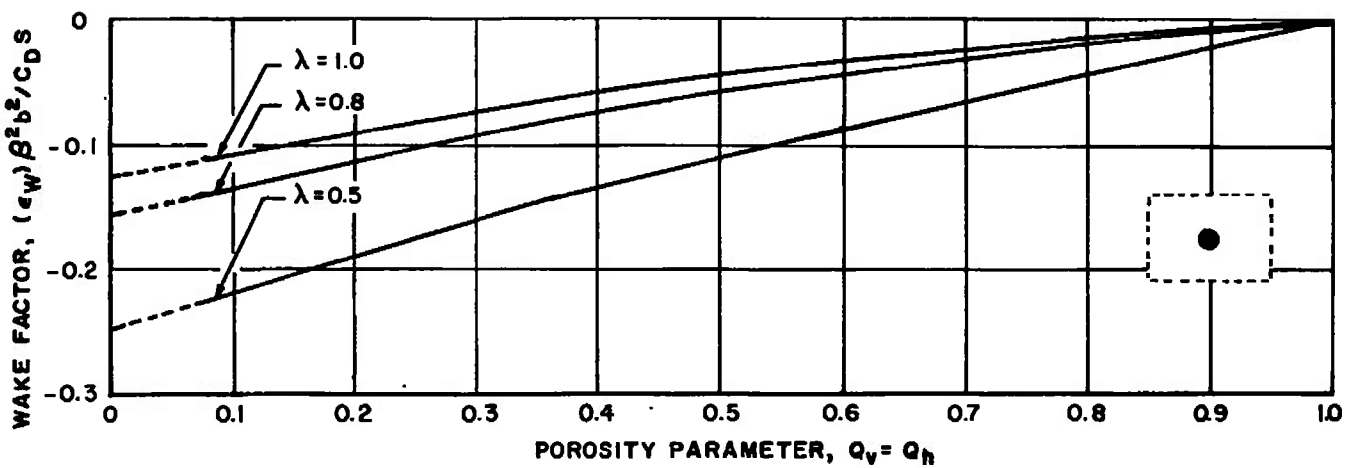

Fig. 7 Wake Blockage Factor at the Model Position for Tunnels with All Walls of Equal Porosity

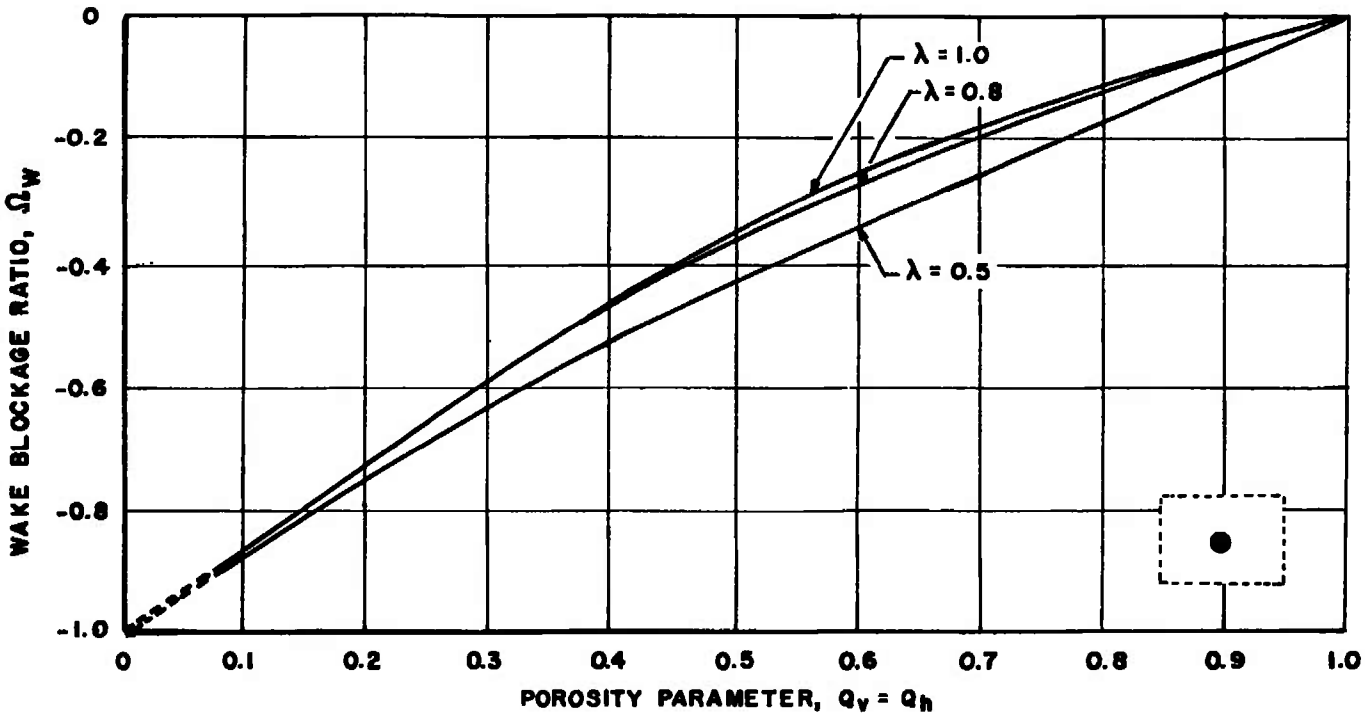

Fig. 8 Wake Bockage Ratio at the Model Position for Tunnels with All Walls of Equal Porosity

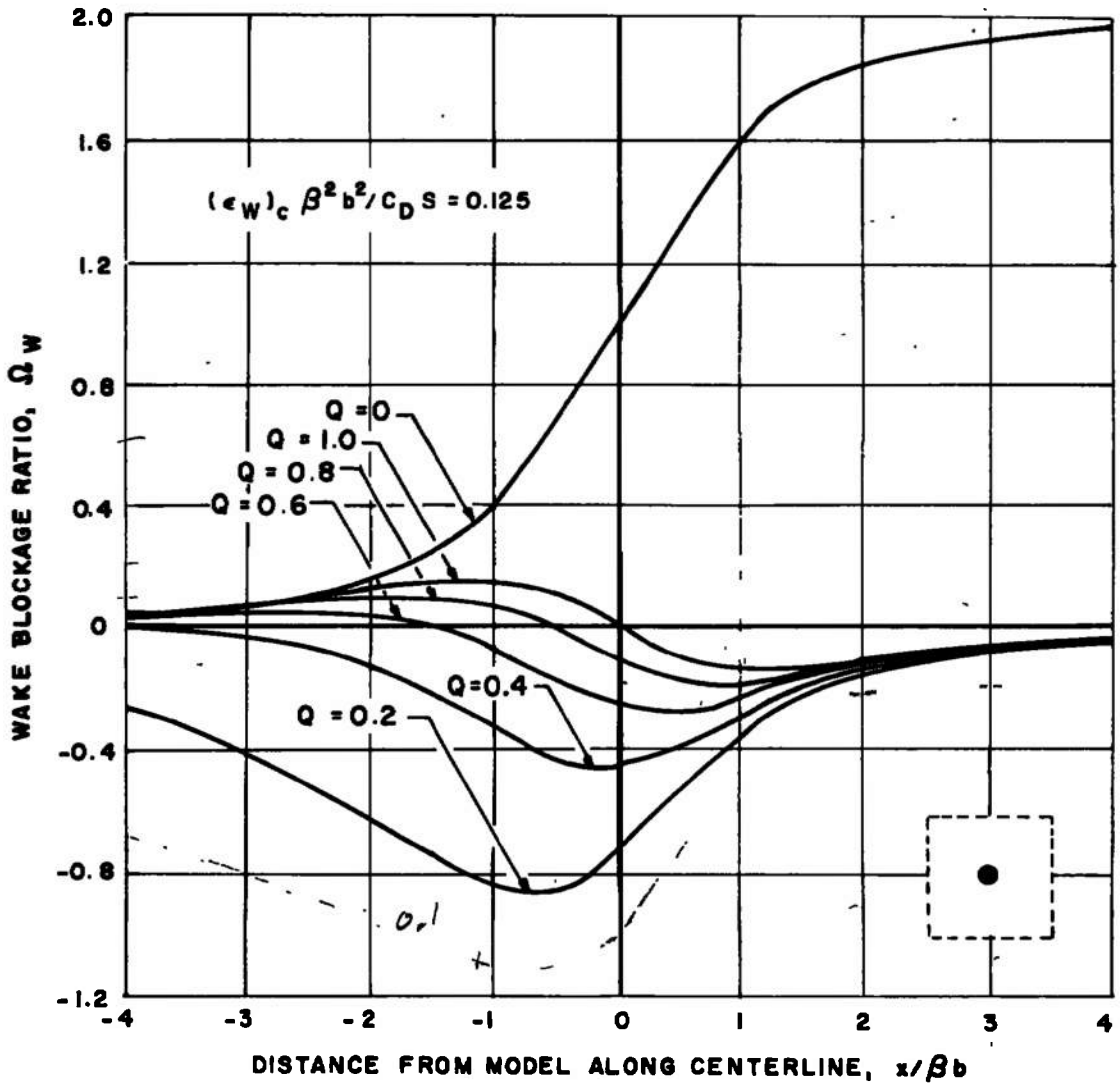

a. $\lambda = 1.0$

Fig. 9 Distribution of the Wake Blockage Ratio along the Centerline of Tunnels with All Walls of Equal Porosity

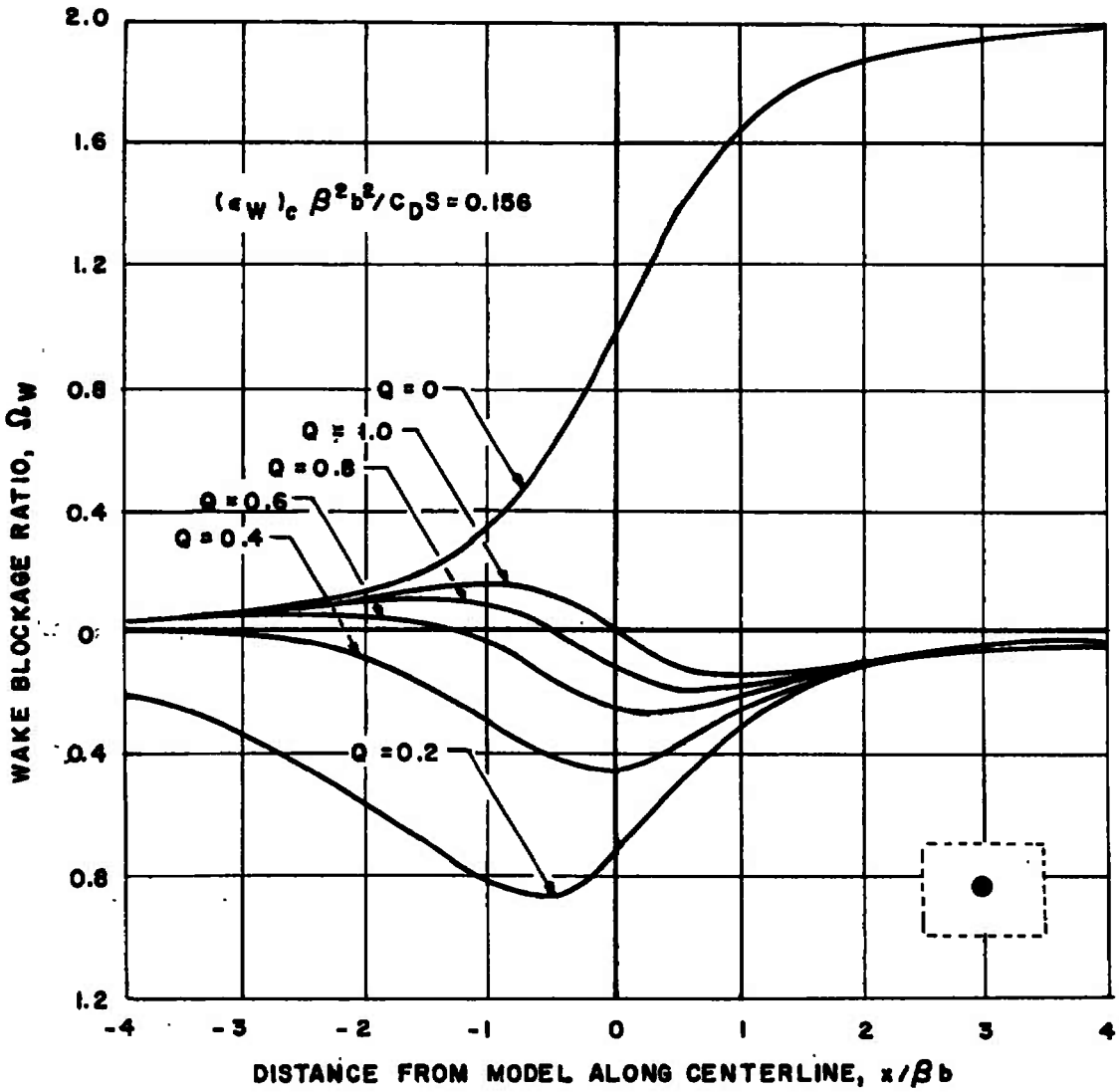

b. $\lambda = 0.8$

Fig. 9 Continued

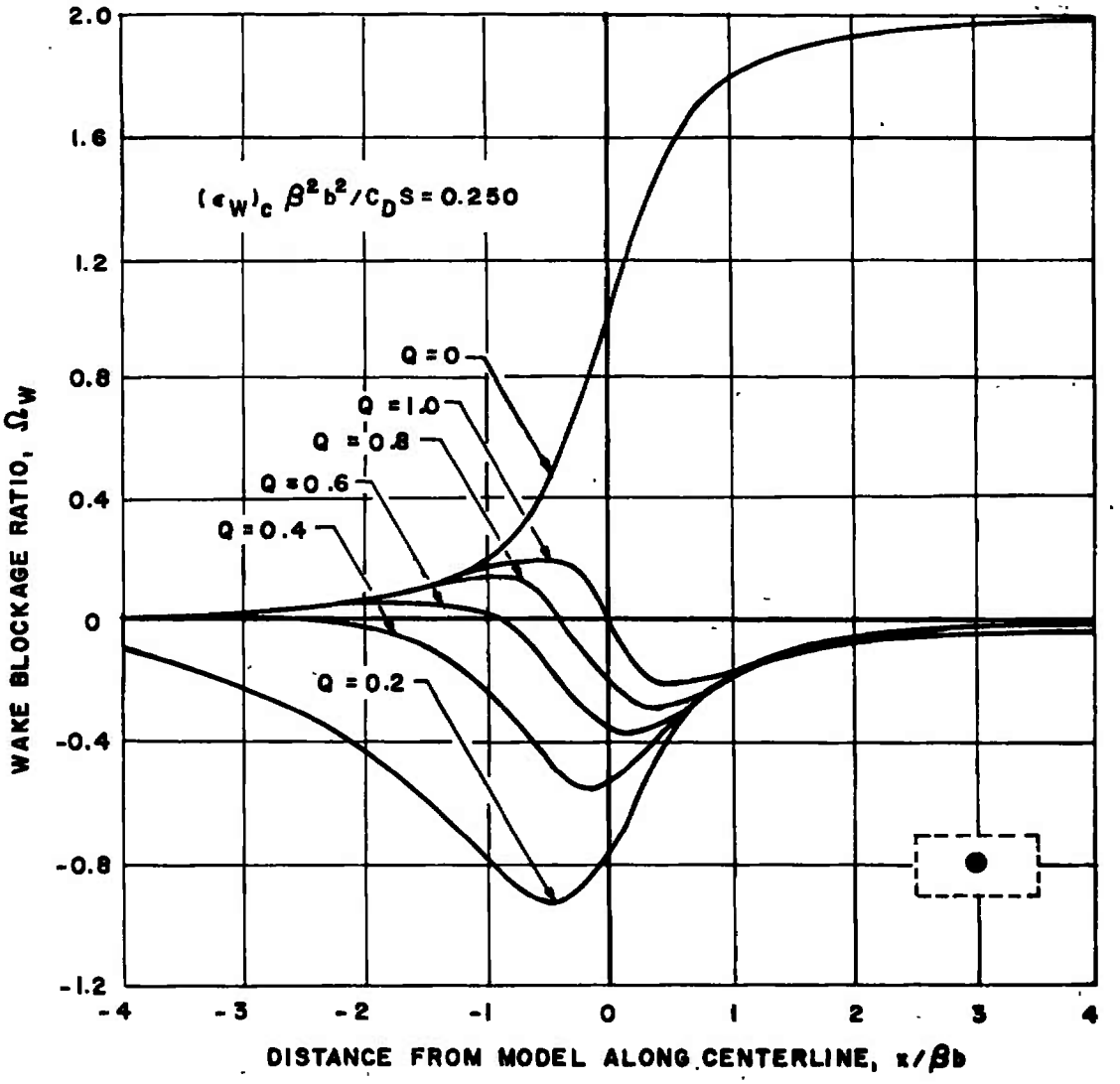

c. $\lambda = 0.5$

Fig. 9 Concluded

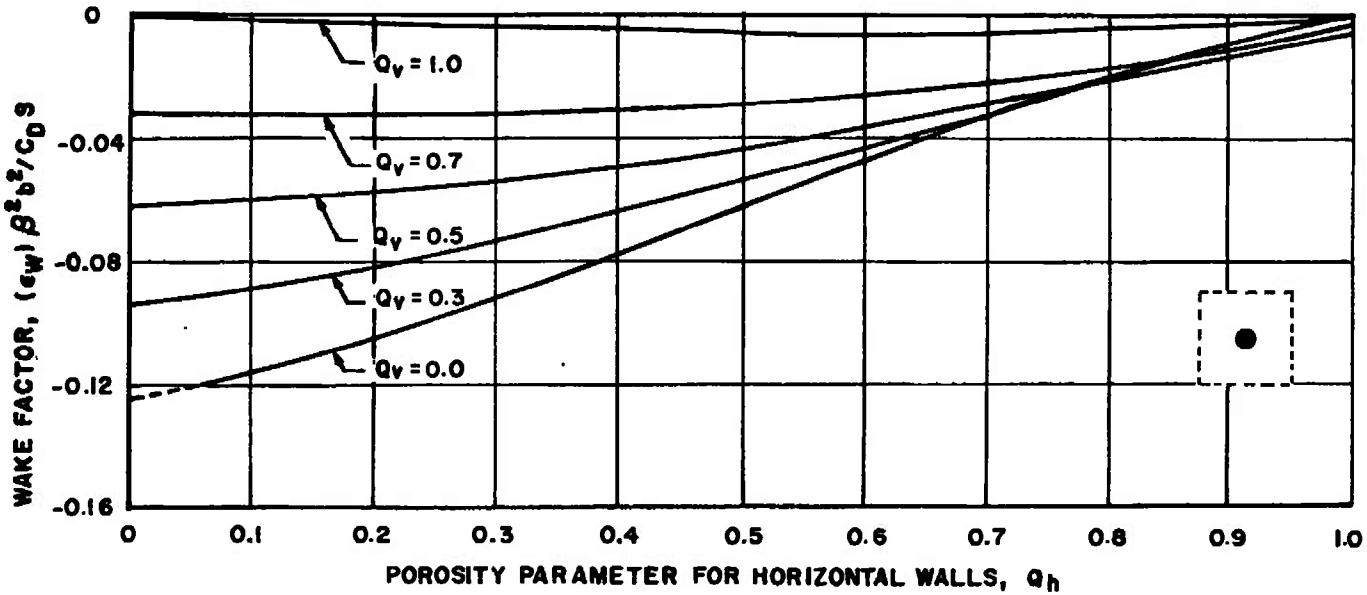

Fig. 10 Wake Blockage Factor at the Model Position versus Q_h for Various Values of Q_v for a Square Tunnel

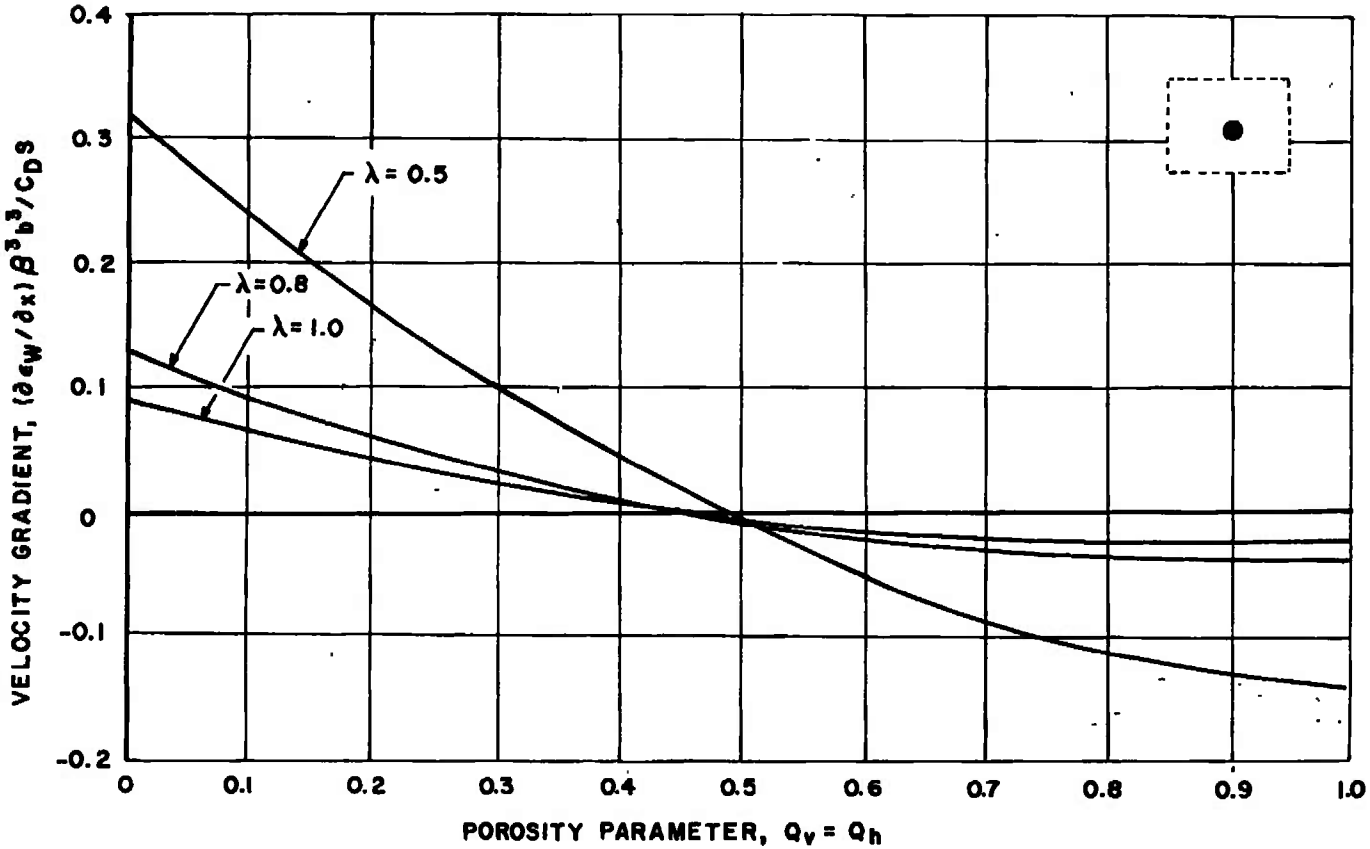

Fig. 11 Wake Blockage Gradient at the Model Position for Tunnels with All Walls of Equal Porosity

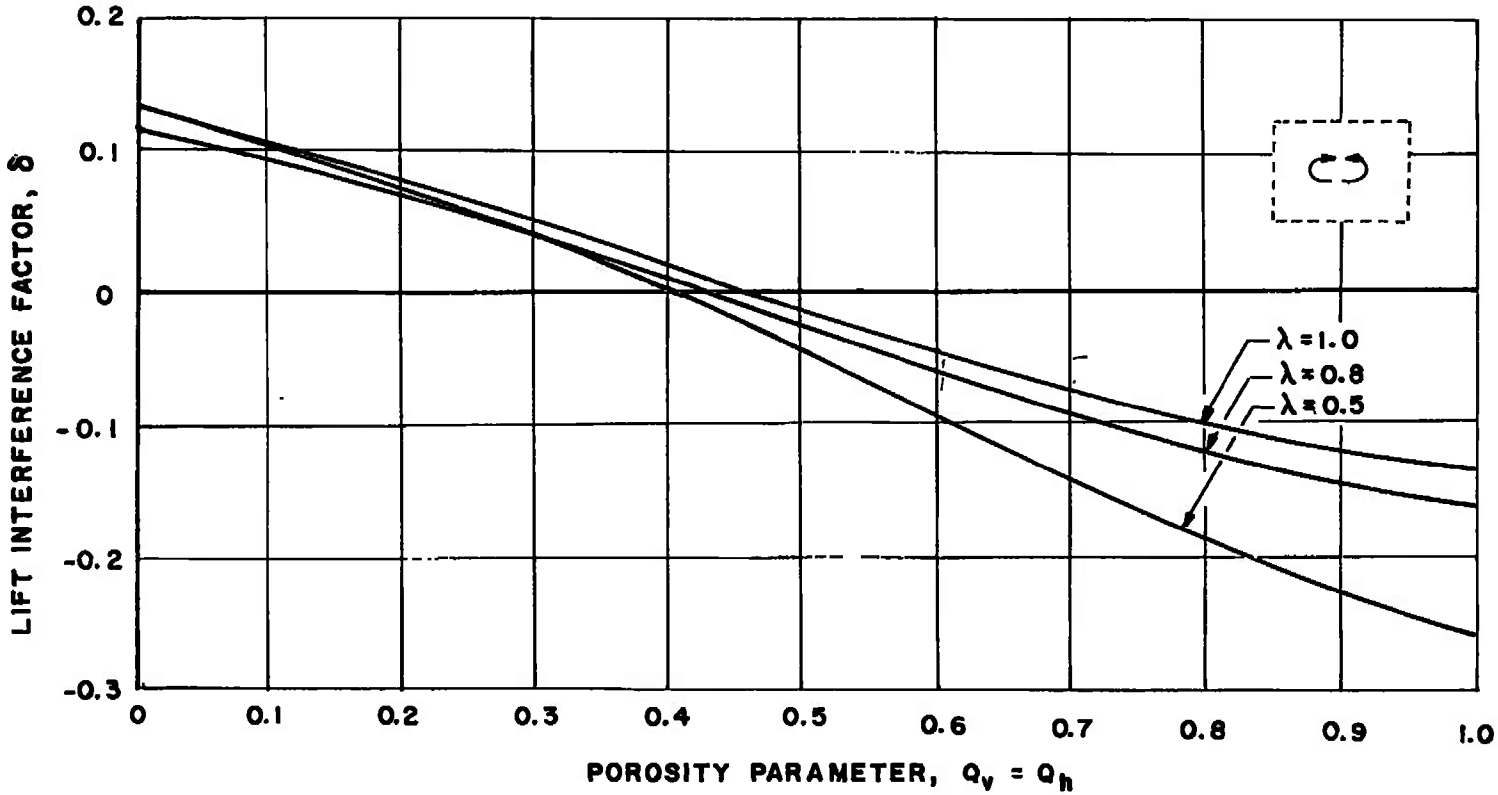

Fig. 12 Lift Interference Factor at the Model Position for Tunnels with All Walls of Equal Porosity

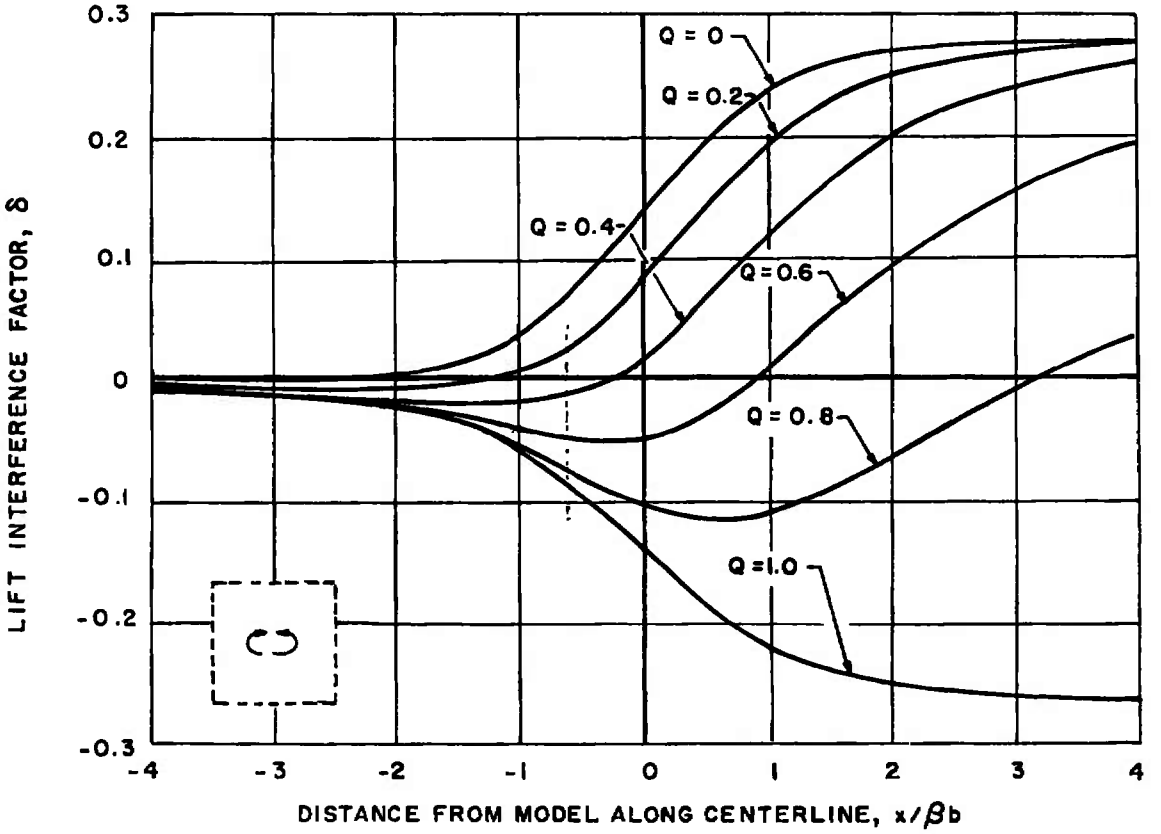

a. $\lambda = 1.0$

Fig. 13 Distribution of the Lift Interference Factor along the Centerline of Tunnels with All Walls of Equal Porosity

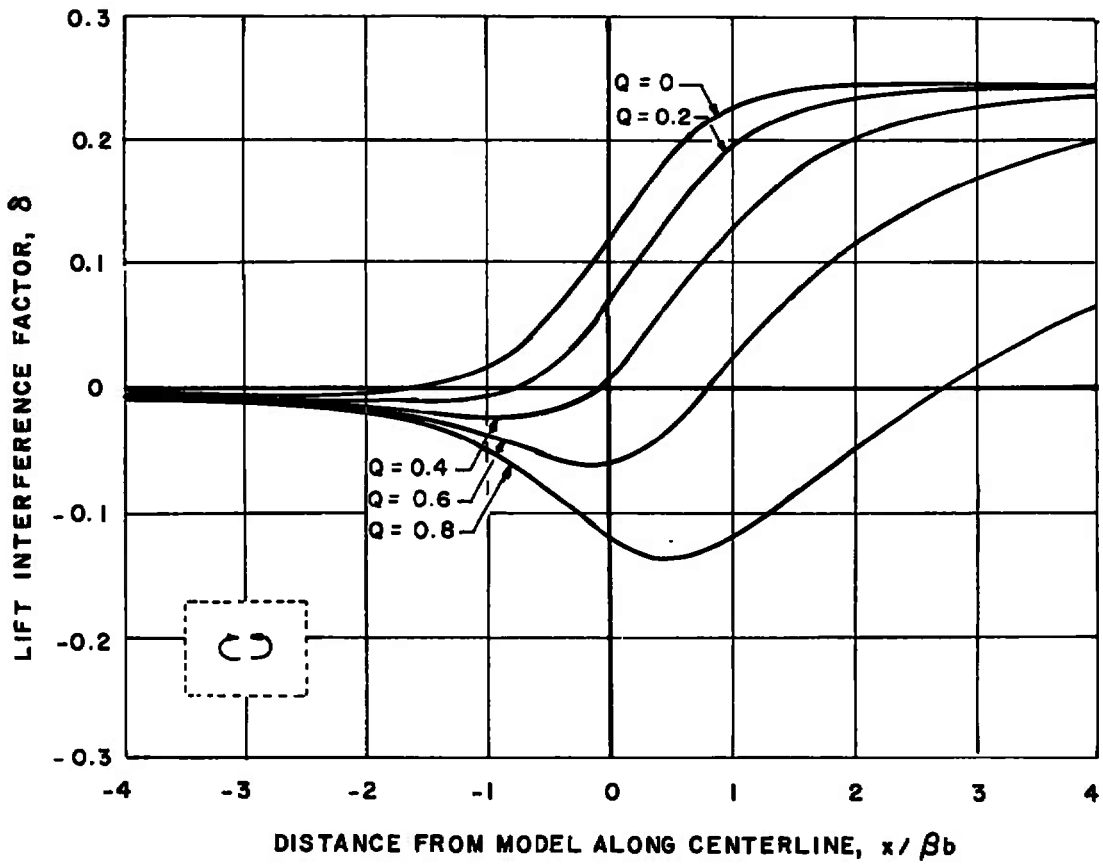

b. $\lambda = 0.8$

Fig. 13 Continued

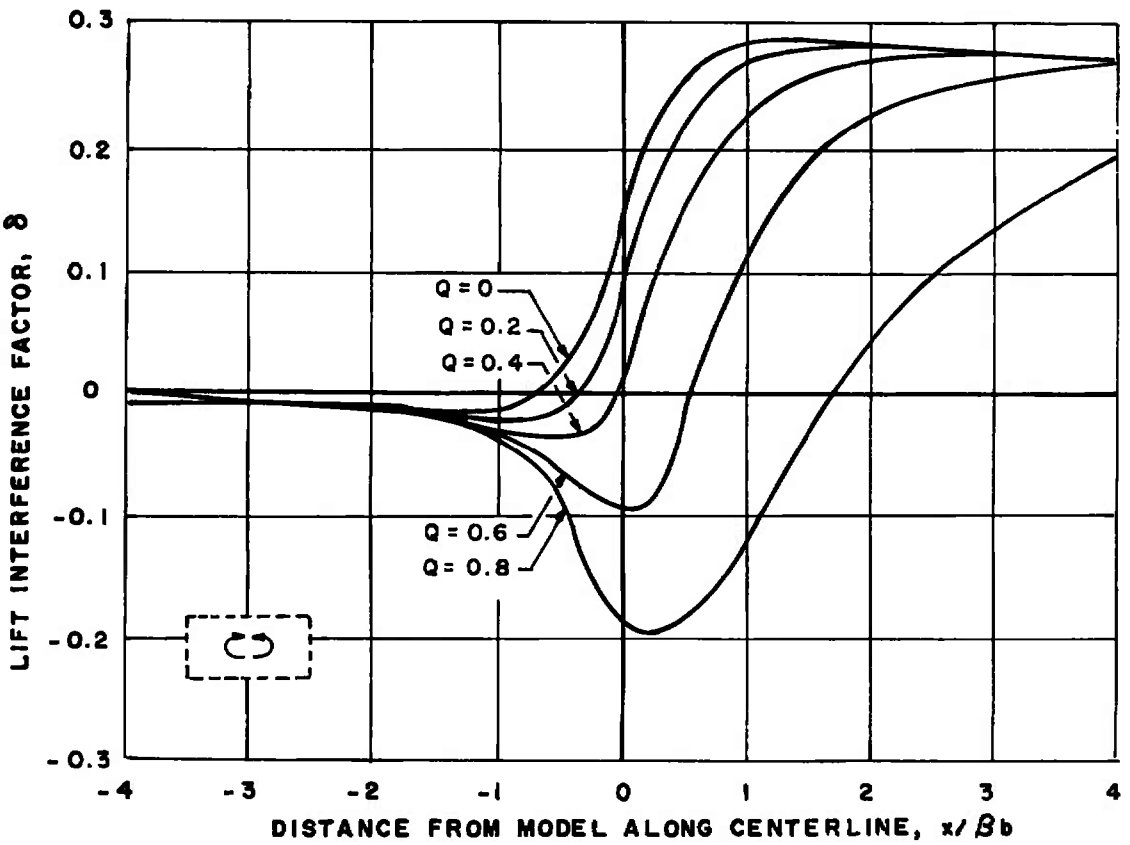

c. $\lambda = 0.5$

Fig. 13 Concluded

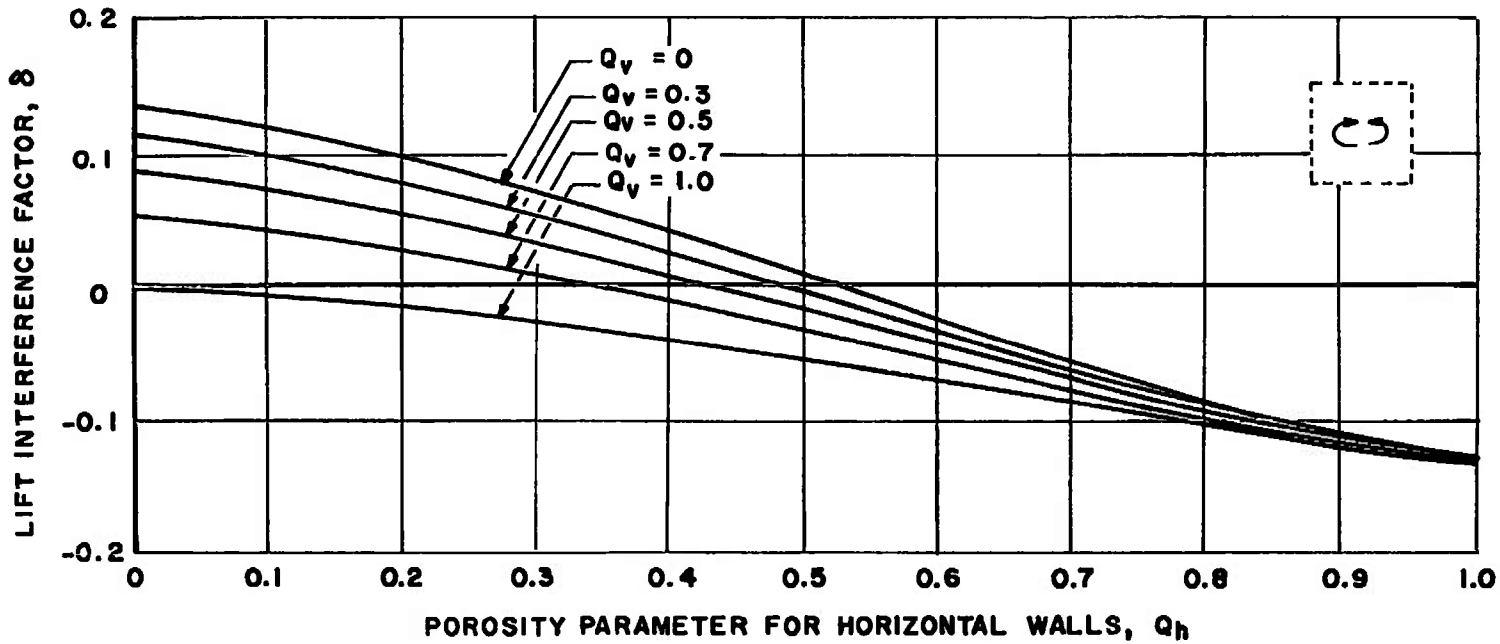

a. $\lambda = 1.0$

Fig. 14 Lift Interference Factor at the Model Position versus Q_h for Various Values of Q_v

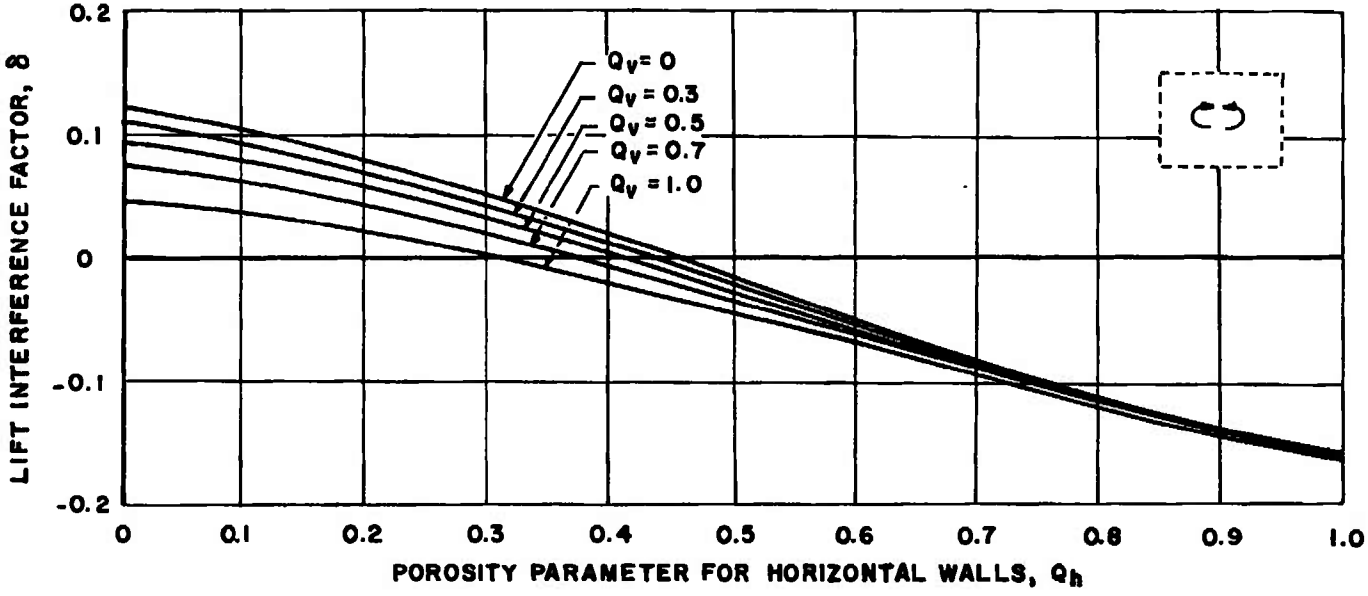

b. $\lambda = 0.8$

Fig. 14 Continued

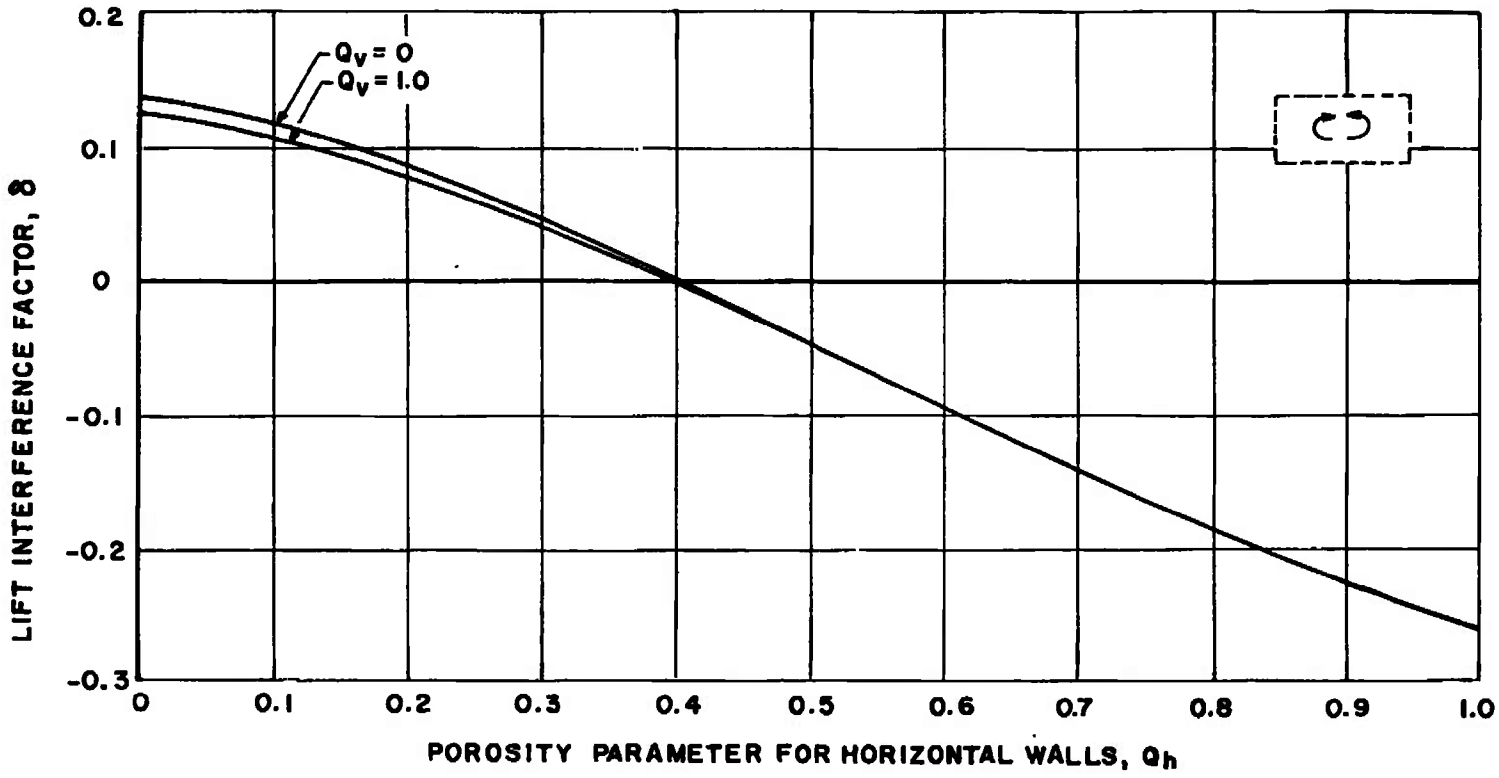

c. $\lambda = 0.5$

Fig. 14 Concluded

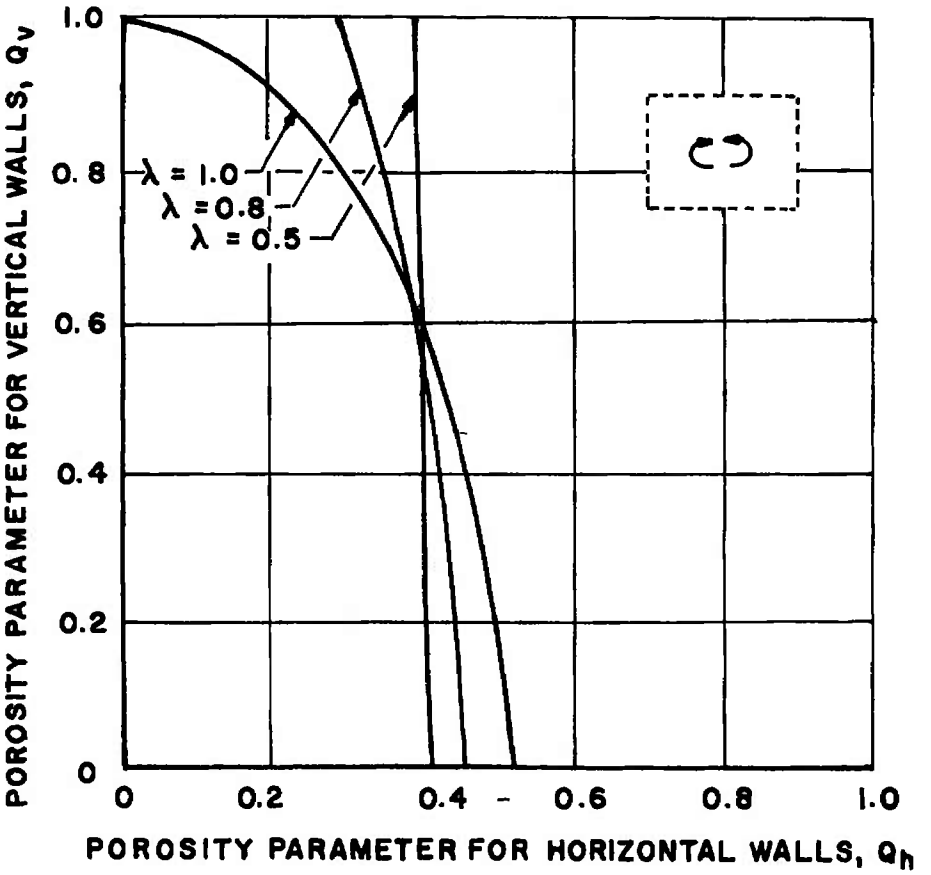

Fig. 15 Zero Lift Interference Curves for Perforated Tunnels

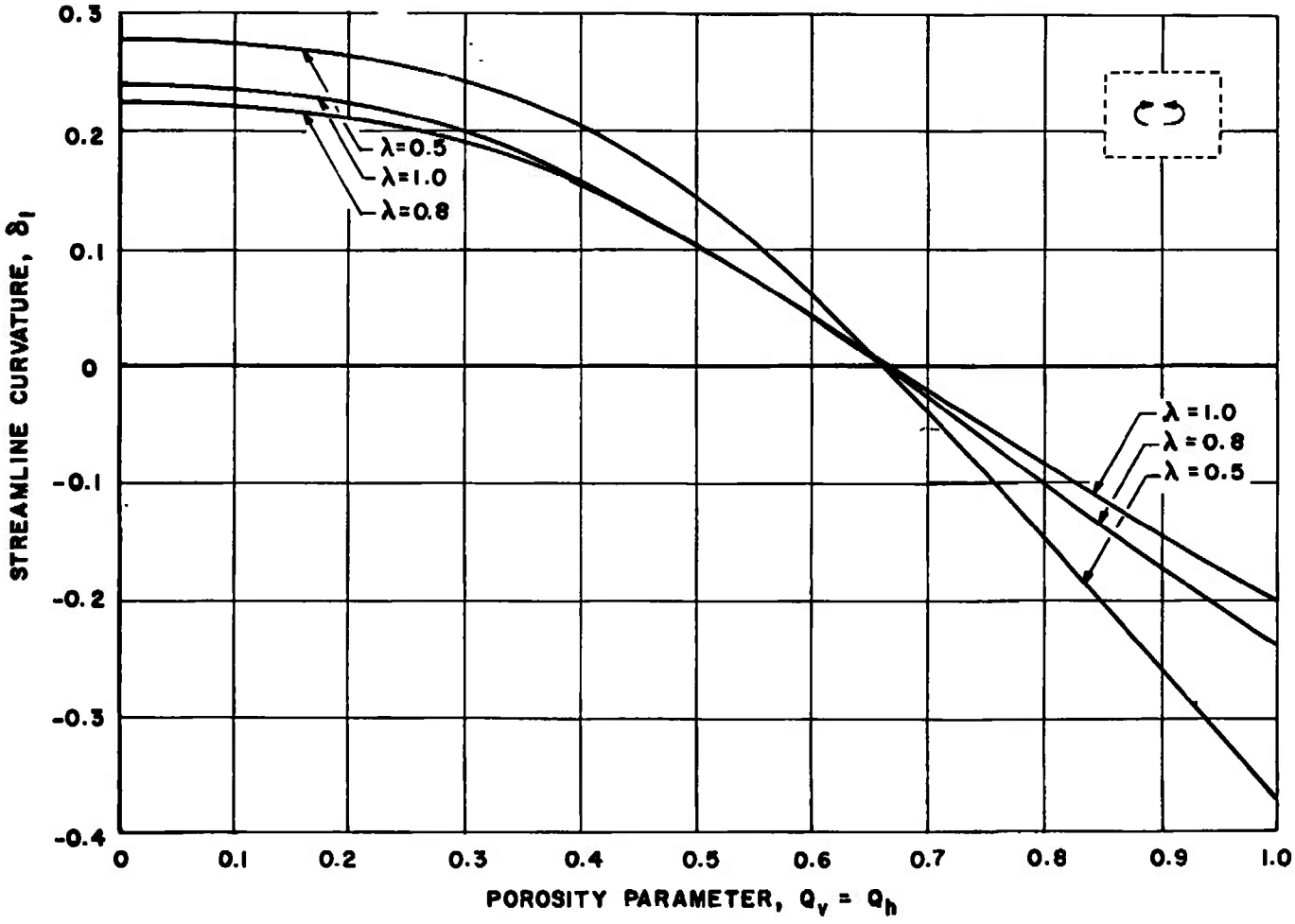

Fig. 16 Streamline Curvature at the Model Position for Tunnels with All Walls of Equal Porosity

UNCLASSIFIED
Security Classification

DOCUMENT CONTROL DATA - R & D

(Security classification of title, body of abstract and indexing annotation must be entered when the overall report is classified)

1. ORIGINATING ACTIVITY *(Corporate author)* Arnold Engineering Development Center ARO, Inc., Operating Contractor Arnold Air Force Station, Tennessee 37389	2a. REPORT SECURITY CLASSIFICATION UNCLASSIFIED 2b. GROUP N/A

3. REPORT TITLE

BOUNDARY INTERFERENCE IN A RECTANGULAR WIND TUNNEL WITH PERFORATED WALLS

4. DESCRIPTIVE NOTES *(Type of report and inclusive dates)*

Final Report January to August 1969

5. AUTHOR(S) *(First name, middle initial, last name)*

C. F. Lo and R. H. Oliver, ARO, Inc.

6. REPORT DATE	7a. TOTAL NO. OF PAGES	7b. NO. OF REFS
April 1970	51	8

8a. CONTRACT OR GRANT NO.	9a. ORIGINATOR'S REPORT NUMBER(S)
F40600-69-C-0001 b. PROJECT NO. A106 c. Program Element 63101F d.	AEDC-TR-70-67 9b. OTHER REPORT NO(S) *(Any other numbers that may be assigned this report)* N/A

10. DISTRIBUTION STATEMENT

This document has been approved for public release and sale; its distribution is unlimited.

11. SUPPLEMENTARY NOTES	12. SPONSORING MILITARY ACTIVITY
Available in DDC.	Arnold Engineering Development Center, AFSC, Arnold Air Force Station, Tennessee 37389

13. ABSTRACT

The boundary interference at subsonic speeds is presented for rectangular wind tunnels with perforated walls. The point-matching method is used for the analysis with an equivalent homogeneous boundary condition at the perforated walls. Numerical results are given for rectangular wind tunnels having various porosities and height-to-width ratios of 1.0, 0.8, and 0.5.

DD FORM 1 NOV 65 1473

UNCLASSIFIED
Security Classification

14. KEY WORDS	LINK A		LINK B		LINK C	
	ROLE	WT	ROLE	WT	ROLE	WT
boundary layer						
subsonic wind tunnels						
wakes						
blocking						
test facilities						